

## NEUROSCIENCE

# Neuronal circuit mechanisms of competitive interaction between action-based and coincidence learning

Eyal Rozenfeld<sup>1,2</sup> and Moshe Parnas<sup>1,2\*</sup>

**How information is integrated across different forms of learning is crucial to understanding higher cognitive functions. Animals form classic or operant associations between cues and their outcomes. It is believed that a prerequisite for operant conditioning is the formation of a classical association. Thus, both memories coexist and are additive. However, the two memories can result in opposing behavioral responses, which can be disadvantageous. We show that *Drosophila* classical and operant olfactory conditioning rely on distinct neuronal pathways leading to different behavioral responses. Plasticity in both pathways cannot be formed simultaneously. If plasticity occurs at both pathways, interference between them occurs and learning is disrupted. Activity of the navigation center is required to prevent plasticity in the classical pathway and enable it in the operant pathway. These findings fundamentally challenge hierarchical views of operant and classical learning and show that active processes prevent coexistence of the two memories.**

Copyright © 2024 The Authors, some rights reserved; exclusive licensee American Association for the Advancement of Science. No claim to original U.S. Government Works. Distributed under a Creative Commons Attribution NonCommercial License 4.0 (CC BY-NC).

## INTRODUCTION

How information is integrated across different forms of learning is crucial to understanding higher cognitive functions. Learning to associate cues with outcomes, either positive or negative, is a crucial adaptive process. When a cue consistently predicts an outcome regardless of an individual's behavior, a classical (Pavlovian) conditioning association is formed. In contrast, when an individual's actions directly influence the occurrence of an outcome, an operant (instrumental, Thorndikian) conditioning occurs (1, 2). Classical and operant conditioning are distinct forms of learning and involve different brain structures (1, 3–5). Furthermore, it is believed that during operant conditioning, the classical conditioning pathway may also be recruited as the environmental stimuli and reinforcers are similar in both cases (6, 7). It is believed that classical conditioning is a prerequisite to operant conditioning (6). According to this two-step process theory, classical and operant conditioning are believed to be additive (6). However, because of the different context, classical and operant conditioning can result in different behavioral responses even if the environmental stimuli and reinforces are similar (8, 9). Thus, a conflict between the two pathways may result in an inadequate behavioral response to a salient cue. Furthermore, according to the two-step process, classical conditioning should be formed under similar conditions as operant conditioning; however, it is well documented that operant memories can be formed under conditions that do not generate classical memories (10). Despite decades of research on classical and operant learning, the interplay between their underlying neuronal circuits remains poorly understood. In particular, how exposure to the same external stimuli (e.g., cue + punishment) can lead to diverging memories and cognitive processes is still unknown. Furthermore, how an individual's operant actions affect the instrumental learning process remains elusive.

*Drosophila* is an ideal model system to address these questions due to its unparalleled genetic access to neurons and relatively simple brain. *Drosophila* has served as a valuable model system for studying classical conditioning for decades, substantially contributing

to our understanding of the underlying mechanisms of learning and memory (11, 12). However, while behavioral evidence suggests that flies can perform operant learning (10, 13–25), little is known about the underlying neuronal circuit and its interaction with the neuronal circuit underlying classical conditioning.

One of the most studied classical learning and memory processes in *Drosophila* is associative olfactory learning and memory. In *Drosophila* olfactory learning, sensory and reinforcement signals converge at axons of third-order Kenyon cells (KCs), constituting the principal neurons of the mushroom body (MB) (26–29). The output of KCs is read by MB output neurons (MBONs) (26, 29, 30), and dendrites of each type of MBON occupy a specific subregion of the MB lobes (26, 29, 31). The reinforcing signal is provided by the axons of dopaminergic neurons (DANs) (14, 32–34). Like MBONs, the axonal arborization of each DAN is restricted to a specific subregion along the MB lobes (26, 29, 31). The coincidence of dopaminergic neuromodulation with an odor stimulus results in long-term depression (LTD) of the KC-MBON synapses, forming the basis for associative learning (35–39).

Here, we show that following olfactory operant conditioning, flies display a different behavioral response in comparison to the behavioral response following classical conditioning. Operant conditioning occurs at the MB neural circuit and requires LTD of the KC-MBON synapse but, like vertebrates, involves a different circuit than that of classical conditioning. Strikingly, and in contrast to the current dogma, we show that plasticity in the operant and classical learning pathways is mutually exclusive such that operant and classical memories cannot be formed at the same time. Furthermore, if plasticity occurs at both pathways, this results in interference between the pathways and no learning is observed. We find that the central complex (CX), the navigation center of *Drosophila*, is required for operant conditioning. Further, we show that the CX undergoes plasticity following operant learning and that CX neurons that are active during the operant task increase their response to the conditioned odor. CX activity gates the separation between the operant and classical learning neuronal pathways, and in the absence of CX activity, following operant conditioning, LTD is observed also in KC-MBON synapses that belong to the classical learning pathway.

<sup>1</sup>Department of Physiology and Pharmacology, Faculty of Medical and Health Sciences, Tel Aviv University, Tel Aviv 69978, Israel. <sup>2</sup>Sagol School of Neuroscience, Tel Aviv University, Tel Aviv 69978, Israel.

\*Corresponding author. Email: mparnas@tauex.tau.ac.il

**RESULTS****Operant and classical conditioning results in conflicting behavioral strategies**

Since to date, only one paper demonstrated operant learning in *Drosophila* in the context of aversive olfactory learning (14), we initially sought to replicate this behavior in the same behavioral setup, which is well characterized for testing classical aversive olfactory learning and fly behavior (14, 40–45). Flies were simultaneously exposed to

two odors, 3-octanol [3-oct, conditioned stimulus ( $CS^-$ )] on one side and 4-methylcyclohexanol (MCH,  $CS^+$ ) on the other side of the behavioral chamber for 2 min (Fig. 1A). This was followed by two training sessions of 2 min that were 5 min apart. In each training session, MCH was presented only in one-half of the chamber (see Materials and Methods). A fly received electric shocks upon entry to the side of the chamber with MCH and throughout its duration there (Fig. 1A). Last, the flies' preference to the  $CS^+$  and  $CS^-$  was

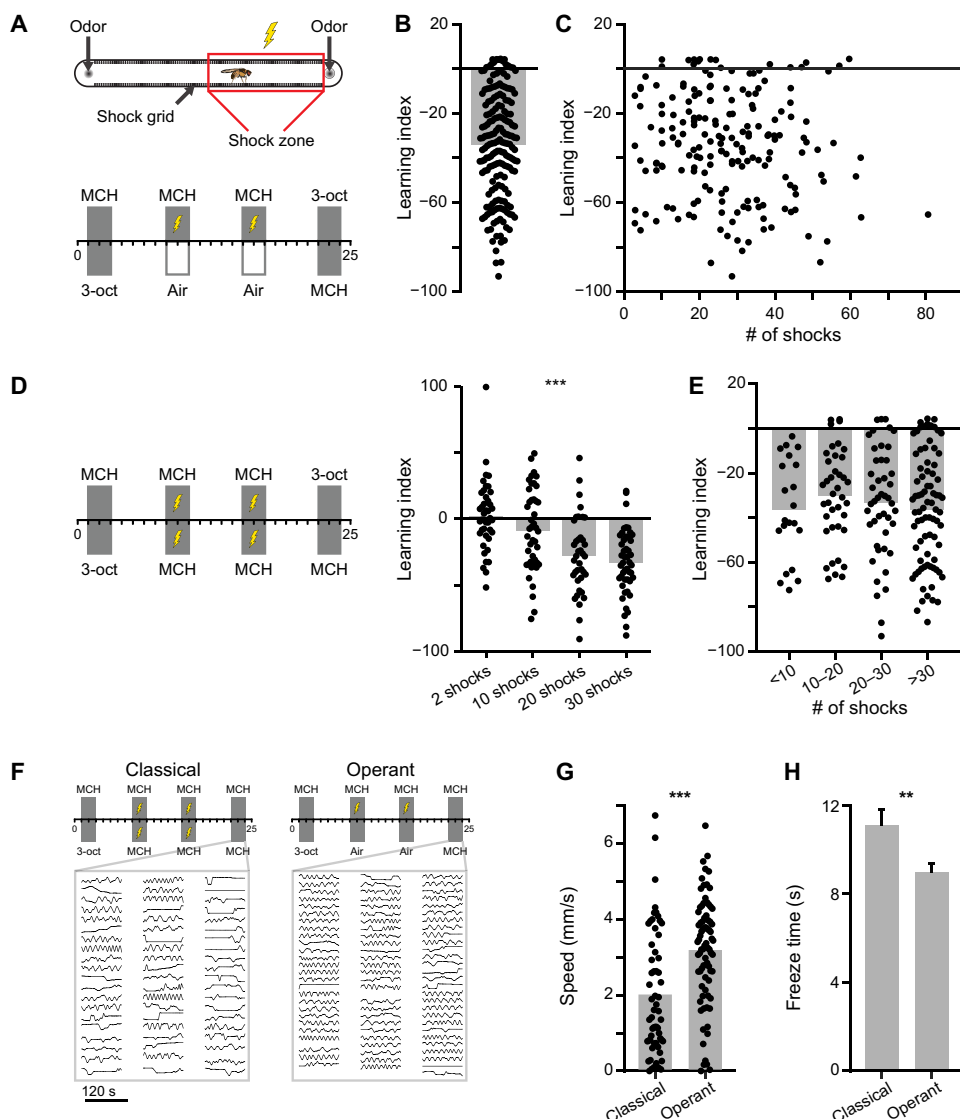


**Fig. 1. Flies perform aversive olfactory operant learning.** (A) Experimental protocol. The  $CS^+$  (MCH) was presented in one side of the chamber and  $CS^-$  (3-oct) in the other side. After 5 min, during acquisition, entering the  $CS^+$  side triggered an electric shock. After two training sessions, the flies were tested with  $CS^+$  and  $CS^-$  during the retrieval phase. (B) *wt* flies learning index following operant conditioning with negative values representing  $CS^+$  aversion ( $N = 162$ ). (C) Number of shocks versus the learning index for the data in (B). No correlation was observed between the number of shocks and the learning index. (D) Left, experimental protocol. Flies were initially presented with  $CS^+$  (MCH) in one side of the chamber and  $CS^-$  (3-oct) in the other half. After 5 min, during acquisition,  $CS^+$  was presented on both sides with electrical shocks. After two training sessions, the flies were tested with  $CS^+$  and  $CS^-$  during retrieval. Right, classical learning in *wt* flies where the  $CS^+$  (MCH) was paired with 2 ( $N = 41$ ), 10 ( $N = 44$ ), 20 ( $N = 38$ ), or 30 ( $N = 47$ ) electrical shocks. Learning is improved with the increase in the number of shocks. (E) Operant learning performance [from data in (C)] in *wt* flies was binned to less than 10 shocks, 10 to 20 shocks, 20 to 30 shocks, and more than 30 shocks. Operant learning did not improve with the increase in the number of electrical shocks. (F) Top, *wt* flies underwent classical (left) or operant (right) training, with  $CS^+$  on both sides during retrieval. Bottom, individual fly positions over time in the chamber during retrieval. (G) Average speed during the retrieval phase for operant ( $N = 80$ ) and classical ( $N = 60$ ) conditioning. (H) Average freeze duration during the retrieval phase for classical ( $N = 2446$  events) or operant ( $N = 3713$  events) conditioning. Error bars are SEM. Dots represent single flies. \*\* $P < 0.01$ , \*\*\* $P < 0.001$ , for statistical analysis, see table S1.

tested (Learning index). Following this operant conditioning protocol, robust learning was observed (Fig. 1B). Flies' operant learning was observed irrespective of the odor used as flies also exhibited operant learning when 3-oct was used as the CS<sup>+</sup> and MCH as the CS<sup>-</sup> (fig. S1A). It is possible that since the electric shock was delivered in one half of the chamber, flies associated the location rather than the odor itself with the electric shock. However, the ability to learn was independent of the location of the CS<sup>+</sup> in the chamber (fig. S1B). In addition, flies did not use a place learning strategy since flies did not learn to avoid the location that was associated with a shock if it was not paired with an odor (fig. S1D). In addition, flies did not change their odor valence when no odor was presented in the training sessions (fig. S1, E and G). In the current training protocol, flies are exposed for a longer time to the conditioned odor (MCH) than to the reference odor (3-oct). However, this longer exposure does not change MCH odor valence (fig. S1, F and G). It was previously shown that flies form an appetitive safety memory upon the cessation of the electric shock (46, 47). Thus, it is possible that rather than forming an aversive association to the CS<sup>+</sup>, flies generated an appetitive safety memory. However, flies did not form an appetitive safety memory for leaving the CS<sup>+</sup> area as testing the reference odor, 3-oct, against a third odor isoamyl acetate did not show any attraction to 3-oct (fig. S1C). Furthermore, blocking synaptic release from the reward encoding dopaminergic protocerebral anterior medial (PAM) cluster neurons did not affect learning (fig. S1H). Last, in contrast to classical conditioning (Fig. 1D), which is ineffective with low number of electric shocks (two shocks, Fig. 1D) and strengthen as the number of electric shocks is increased (Fig. 1D) (48, 49), in operant conditioning, consistent with previous reports (10), there was no correlation between the number of electrical shocks a fly received to its learning index, and even two electric shocks were sufficient to drive conditioning (Fig. 1, C and E, and fig. S1I). Together, the operant conditioning assay forms a robust association between the unconditioned stimulus (US) and the CS (i.e., odor shock).

In both the operant and classical learning paradigms, an odor is paired with an electrical shock. Nevertheless, operant and classical conditioning may result in different behavioral strategies. For example, following classical conditioning, mice freeze when exposed to the CS<sup>+</sup>, but following operant learning, they show active avoidance of the CS<sup>+</sup> (8, 9). To examine whether flies show different behavioral phenotypes following classical and operant learning, we trained wild-type (*wt*, *w<sup>1118</sup>* flies) flies in the operant or classical paradigm and presented the CS<sup>+</sup> in both sides of the chamber in the retrieval phase (Fig. 1F). Flies displayed a different behavioral response to the CS<sup>+</sup> following classical or operant learning (Fig. 1, G and H). Following classical learning, flies showed an increase in freezing behavior and reduced walking speed compared to flies that underwent operant learning (Fig. 1, G and H). The increase in freezing was also observed when the CS<sup>+</sup> was 3-oct (fig. S2, A and B) and did not occur when no shock or no odor were provided during training (fig. S2, C and D). Thus, flies can perform operant aversive olfactory learning, which requires fewer presentations of the negative reinforcer than classical aversive olfactory learning. These data also show that following operant and classical learning, flies use different behavioral strategies upon encounter of the CS<sup>+</sup>. Together, these results may suggest that different neural circuits underlie operant and classical conditioning.

## The MB neural circuit is required for operant learning

In an attempt to find the neural circuit underlying operant conditioning in flies, we systematically silenced neurons of interest and examined the effect such silencing had on operant learning and memory. The MB is considered to be the main locus of classical aversive olfactory learning (11, 12, 50), where different populations of KCs are responsible for forming many varieties of classical aversive learning (30, 51–61). To test whether KCs are involved in operant learning, we blocked synaptic release from all KC neurons in the MB using the GAL4/UAS system and the *shibire<sup>ts1</sup>* (*shi<sup>ts1</sup>*) allele that blocks synaptic release at temperatures exceeding 30°C (Fig. 2A) (62). Blocking synaptic release from all KCs completely blocked the formation of operant memories (Fig. 2B). Blocking synaptic release of γ KCs, which play a key role in classical learning (fig. S3), did not affect operant learning (fig. S4A). Similarly, blocking synaptic release from αβ KCs did not affect operant learning (fig. S4B). Only blocking the release of α'β' or of αβ together with the γ KCs disrupted the formation of operant learning (Fig. 2B). Performing the same experiment but at the permissive temperature of 23°C (fig. S5A) that does not block synaptic release had no effect on behavior (fig. S5B). Thus, KCs are required for both operant and classical aversive olfactory conditioning.

In classical conditioning, the US is signaled by activity of DANs (14, 32–34). Two clusters of DANs are involved: the PAM cluster, which is involved in appetitive conditioning, and the protocerebral posterior lateral (PPL) cluster, which underlies aversive conditioning (14, 32–34, 63, 64). We have already verified above that the PAM cluster does not participate in aversive operant conditioning (fig. S1H). Blocking synaptic release from the entire PPL1 cluster abolished operant learning (Fig. 2C). Blocking the synaptic release only from the PPL1-γ1pedc and the PPL1-γ1pedc;α2α'2 subpopulations of PPL1 neurons reduced operant conditioning (Fig. 2C and fig. S5C), whereas PPL1 neurons innervating different regions of the MB did not affect aversive operant conditioning (fig. S4C). In addition to the PPL1 and PAM clusters, the PPL2 dopaminergic cluster was shown to improve classical learning performance (65). Furthermore, PPL2 neurons were also shown to represent movement (66). Thus, they seem to have the capacity to participate in operant learning. However, silencing PPL2 neurons did not affect operant learning (fig. S4D).

In classical aversive olfactory learning, the synapse between KCs and MBONs undergoes synaptic depression that shifts the balance of MBONs driving attraction and aversion to facilitate odor avoidance following learning (30, 35, 60, 67). Furthermore, different MBONs were found to play a role in different learning paradigms (30, 52, 53, 57, 59–61). Therefore, we examined whether a subpopulation of MBONs participates in operant conditioning. Blocking the γ2α'1 (MB077C-GAL4) or the α2sc (MB080C-GAL4) MBONs significantly reduced the formation of operant memories (Fig. 2D and figs. S4E and S5D). To verify that these two MBONs are required for operant conditioning in general, we also performed the operant conditioning when the US was presented on the other half of the chamber and found similar results (fig. S6). Blocking release from these two MBONs did not affect classical learning (Fig. 2E). Furthermore, silencing MBONs that are known to participate in classical conditioning (26) had no effect on operant conditioning (fig. S4E) but did reduce classical conditioning (fig. S3). While blocking MBON-γ2α'1 or MBON α2sc interfered

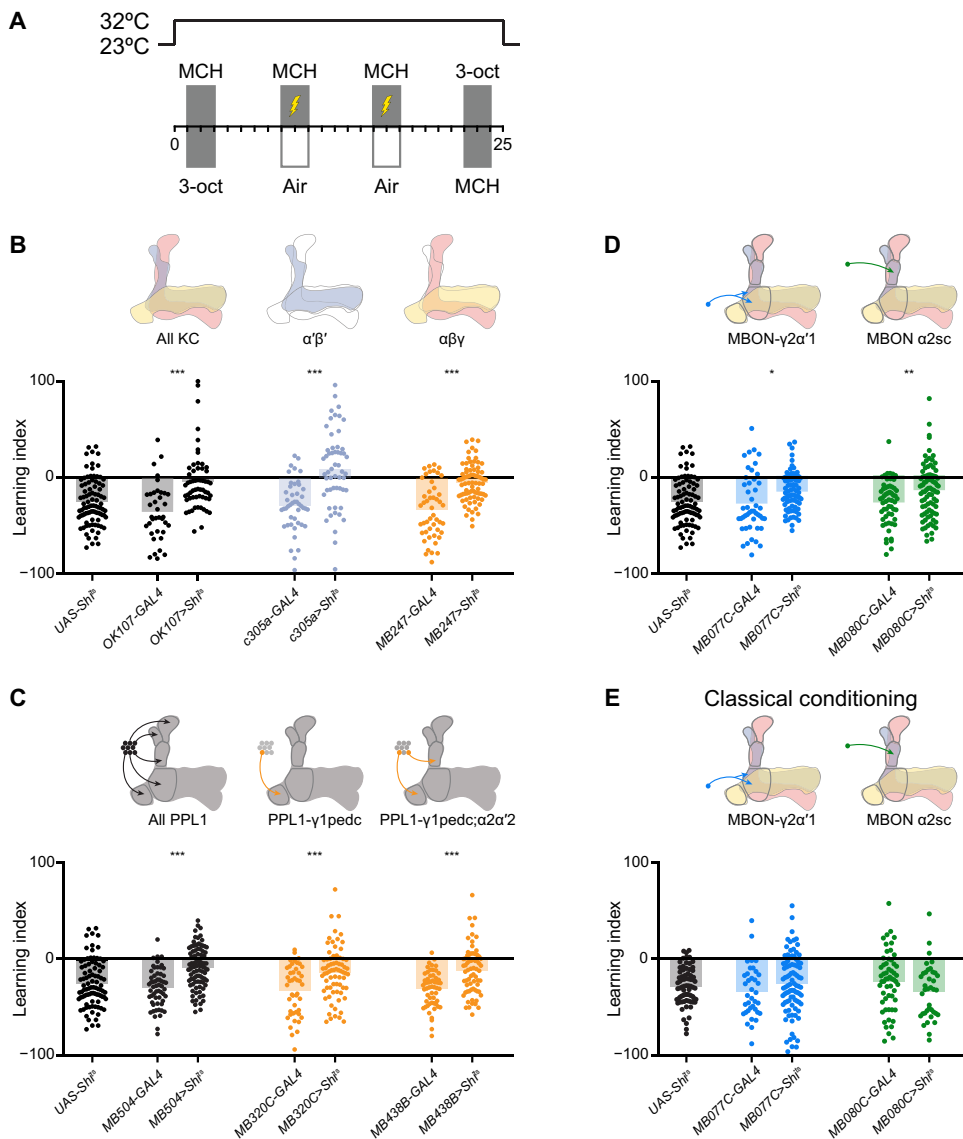


**Fig. 2. MB involvement in operant learning.** **(A)** Experimental protocol. Flies were placed in an incubator set to 32°C 5 min before the start of the experiment. This temperature was maintained throughout the entire experiment, thus blocking synaptic release. **(B)** Blocking synaptic release from all KCs (left: *ok107-GAL4*,  $N = 37$ ; *ok107-GAL4;UAS-shi<sup>ts1</sup>*,  $N = 58$ ; *UAS-shi<sup>ts1</sup>*,  $N = 90$ ),  $\alpha'\beta'$  KCs (middle: *c305a-GAL4*,  $N = 45$ ; *c305a-GAL4;UAS-shi<sup>ts1</sup>*,  $N = 55$ ), and the  $\alpha\beta\gamma$  KCs (right: *MB247-GAL4*,  $N = 48$ ; *MB247-GAL4;UAS-shi<sup>ts1</sup>*,  $N = 78$ ) significantly reduced learning performance in the operant learning task. **(C)** Blocking synaptic release from the PPL1 subpopulation that are punishment encoding DA neurons significantly reduced learning performance in the operant learning task [left: *MB504-GAL4*,  $N = 57$ ; *MB504-GAL4;UAS-shi<sup>ts1</sup>*,  $N = 93$ ; *UAS-shi<sup>ts1</sup>*, the same as in (B)  $N = 90$ ]. Blocking synaptic release from two subpopulations of PPL1 DANs, the PPL1- $\gamma$ 1pedc (middle: *MB320C-GAL4*,  $N = 45$ ; *MB320C-GAL4;UAS-shi<sup>ts1</sup>*,  $N = 72$ ), and the PPL1- $\gamma$ 1pedc; $\alpha$ 2 $\alpha$ '2 (right: *MB438B-GAL4*,  $N = 57$ ; *MB438B-GAL4;UAS-shi<sup>ts1</sup>*,  $N = 68$ ) significantly reduced learning performance in the operant learning task. **(D)** Blocking synaptic release from MBON- $\gamma$ 2 $\alpha$ '1 [left: *MB077C-GAL4*,  $N = 46$ ; *MB077C-GAL4;UAS-shi<sup>ts1</sup>*,  $N = 77$ ; *UAS-shi<sup>ts1</sup>*, the same as in (B)  $N = 90$ ], and MBON- $\alpha$ 2sc (right: *MB080C-GAL4*,  $N = 58$ ; *MB080C-GAL4;UAS-shi<sup>ts1</sup>*,  $N = 88$ ) significantly reduced learning performance in the operant learning task. **(E)** Blocking synaptic release from MBON- $\gamma$ 2 $\alpha$ '1 or the MBON- $\alpha$ 2sc (*MB077C-GAL4*,  $N = 37$ ; *MB077C-GAL4;UAS-shi<sup>ts1</sup>*,  $N = 90$ ; *MB080C-GAL4*,  $N = 57$ ; *MB080C-GAL4;UAS-shi<sup>ts1</sup>*,  $N = 38$ ; *UAS-shi<sup>ts1</sup>*,  $N = 74$ ) did not affect performance in the classical learning task. For all panels, dots represent single flies. \* $P < 0.05$ , \*\* $P < 0.01$ , \*\*\* $P < 0.001$ ; for detailed statistical analysis, see table S1.

with operant conditioning (Fig. 2D), blocking the corresponding PPL1 neurons PPL1- $\gamma$ 2 $\alpha$ '1 or PPL1- $\alpha$ 2 did not disrupt operant conditioning (fig. S4C). However, blocking both PPL1- $\gamma$ 2 $\alpha$ '1 and PPL1- $\alpha$ 2 simultaneously disrupted operant conditioning (fig. S7). It thus appears that in terms of PPL1 activity, it is sufficient to have at least one pathway active (affecting MBON- $\gamma$ 2 $\alpha$ '1 or MBON- $\alpha$ 2sc) for memory formation.

Classical conditioning results in LTD of the KC-MBON synapse (30, 31, 35–37, 39, 59, 60, 68–73) and occurs at the KC presynaptic terminal. Thus, MBON activity is required for memory retrieval. Recently, it was demonstrated that MBON activity is also required for memory acquisition (74). To examine whether operant conditioning shares the same principles, we used *UAS-GtACR2* to express the anion channel rhodopsin GtACR2 (75) and to optogenetically

silence  $\gamma 2\alpha'1$  or  $\alpha 2\text{sc}$  MBONs at precise timing. Silencing MBONs either during the training (fig. S8A) or retrieval (fig. S8B) phases abolished operant learning (fig. S8, C and D). Similar results were also obtained for KCs (fig. S8, E and F). However, for PPL1 neurons, as expected from their role in classical conditioning, their activity was only required during training (fig. S8, G and H). Together, the cumulative results thus far indicate that distinct and parallel neuronal pathways underlie classical and operant conditioning.

### CX is required for olfactory operant learning

The *Drosophila* CX is responsible for flies' navigation capabilities with different populations of neurons encoding a variety of parameters such as heading, velocity, turning and more (76). Previously it was shown that the CX is involved in nonolfactory operant behaviors (77–79) and in olfactory navigation (80–82). Since operant learning relies on the fly's ability to perform a goal directed motor action, namely walking toward the area containing the CS<sup>+</sup> and US, we hypothesized that the CX is involved in this form of learning. We first examined the involvement of ellipsoid body-protocerebral bridge-gall (EPG) neurons, which encode the fly heading (83–89). In accordance with our hypothesis, blocking release from EPG neurons significantly hampered operant learning (Fig. 3). EPG neurons receive input from protocerebral bridge-ellipsoid body-noduli (PEN) neurons, which encodes heading direction and rotational velocity, even when direction cues are not present (88–91). Silencing

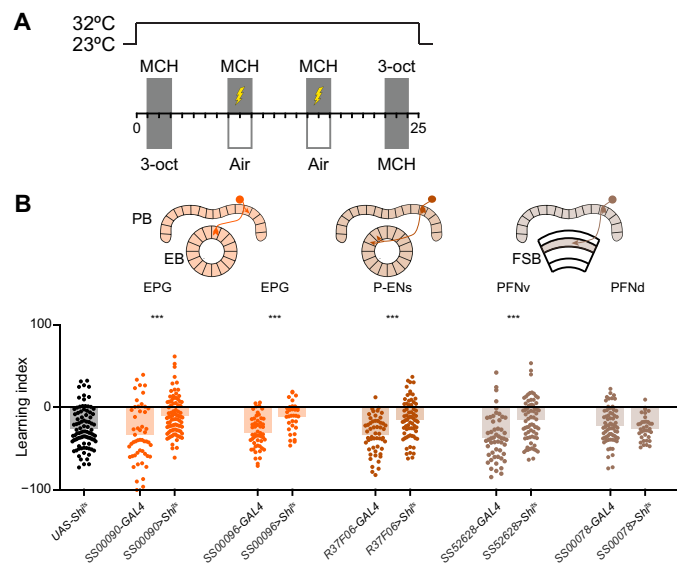


**Fig. 3. CX involvement in operant learning.** (A) Experimental protocol. Flies were placed in an incubator set to 32°C 5 min before the start of the experiment. This temperature was maintained throughout the entire experiment, thus blocking synaptic release. (B) Blocking synaptic release from EPG neurons using two different GAL4 driver lines (*SS0090-GAL4*,  $N = 51$ ; *SS0090-GAL4;UAS-shi<sup>ts1</sup>*,  $N = 89$ ; *SS0096-GAL4*,  $N = 53$ ; *SS0096-GAL4;UAS-shi<sup>ts1</sup>*,  $N = 33$ ; *UAS-shi<sup>ts1</sup>*, the same as in Fig. 2  $N = 90$ ) significantly reduced learning performance in the operant learning task. Blocking synaptic release from P-EN neurons (*R37F06-GAL4*,  $N = 53$ ; *R37F06-GAL4;UAS-shi<sup>ts1</sup>*,  $N = 70$ ) significantly reduced learning performance in the operant learning task. Blocking synaptic release from PFNv neurons (*SS5262-GAL4*,  $N = 53$ ; *SS5262-GAL4;UAS-shi<sup>ts1</sup>*,  $N = 72$ ), but not from PFNd neurons (*SS0078-GAL4*,  $N = 69$ ; *SS0078-GAL4;UAS-shi<sup>ts1</sup>*,  $N = 36$ ), significantly reduced learning performance in the operant learning task. For all panels, dots represent single flies. \*\*\* $P < 0.001$ ; for detailed statistical analysis, see table S1.

PEN neurons also disrupted operant learning (Fig. 3). Blocking synaptic release from EPG and PEN neurons did not affect classical conditioning (fig. S9E) nor the walking speed and the total distance traveled by the flies in the operant task (fig. S9, B and C). We next sought to test the involvement of protocerebral bridge-fanshaped-body-noduli (PFN) neurons in operant learning, which integrate sensory and heading cues to form an egocentric navigational map (92–94). Blocking release from PFNv neurons, which encode backward movement (76), reduced operant learning, while blocking PFNd neurons, which encode forward movement (76), had no effect on operant conditioning (Fig. 3). However, blocking the synaptic release of PFNv neurons also affected classical learning (fig. S9E) and increased the walking speed and the distance traveled (fig. S9, B and C), indicating that their effect is not specific for operant conditioning. Last, EPG and PEN are required during memory acquisition and retrieval (fig. S8, I to L). Thus, the CX is crucial for the formation of memories following operant conditioning by supplying information about the fly heading direction, rotational velocity, and egocentric navigational parameters.

### Operant and classical learning drive plasticity in parallel MBON pathways

The formation of memories following classical aversive olfactory learning relies on synaptic depression between KCs and MBONs (30, 31, 35–37, 39, 59, 60, 68–70, 72, 73), which results in a decreased MBON odor response only to the CS<sup>+</sup>. To examine whether the same mechanism underlies operant learning, we used *in vivo* two-photon functional Ca<sup>2+</sup> imaging. Using the genetically encoded Ca<sup>2+</sup> indicator, GCaMP6f (95), we examined the odor-induced Ca<sup>2+</sup> transients following CS<sup>+</sup> and CS<sup>-</sup> of the MBONs we found to be involved in operant conditioning above. To this end, flies were conditioned in the behavior apparatus and then transferred to the two-photon setup (Fig. 4A). Cold anesthesia within the first 3 hours after conditioning is known to affect fly learning (96); therefore, we initially tested MBON odor responses 3 hours after training. Under these conditions, we observed a decrease in the response to the CS<sup>+</sup> only in the  $\alpha 2\text{sc}$ -MBON (Fig. 4, B and D). However, when we tested flies immediately after the training protocol, only the  $\gamma 2\alpha'1$ -MBON showed decreased CS<sup>+</sup> responses (Fig. 4, B and D). The lack of immediate observed plasticity in  $\alpha 2\text{sc}$ -MBON (Fig. 4B) is not an indication that such plasticity does not occur under physiological conditions. This is because we used cold anesthesia, which could impair memory. We did not observe any changes in CS<sup>+</sup> or CS<sup>-</sup> induced odor responses in both  $\alpha 2\text{sc}$ -MBON and  $\gamma 2\alpha'1$ -MBON when flies underwent classical conditioning (Fig. 4, C and E). Thus, these results are consistent with the behavioral results above (Fig. 2, D and E) showing the involvement of  $\alpha 2\text{sc}$ - and  $\gamma 2\alpha'1$ -MBONs in operant conditioning.

Thus far, we have shown that operant conditioning involves a different neural pathway than classical conditioning. Further, the two different pathways, i.e., classical and operant conditioning, can result in different behavioral output (Fig. 1, G and H). Since the conditions for classical conditioning are embedded within operant conditioning, i.e., an odor is coupled with an electric shock, we examined whether following operant-conditioning plasticity also occurs in the classical learning pathway. To this end, we tested odor responses of the  $\gamma 1\text{pedc} > \alpha/\beta$ -MBON (*MB085C-GAL4*), which was previously shown to undergo synaptic depression following classical learning (35–37, 39). As previously reported, following classical

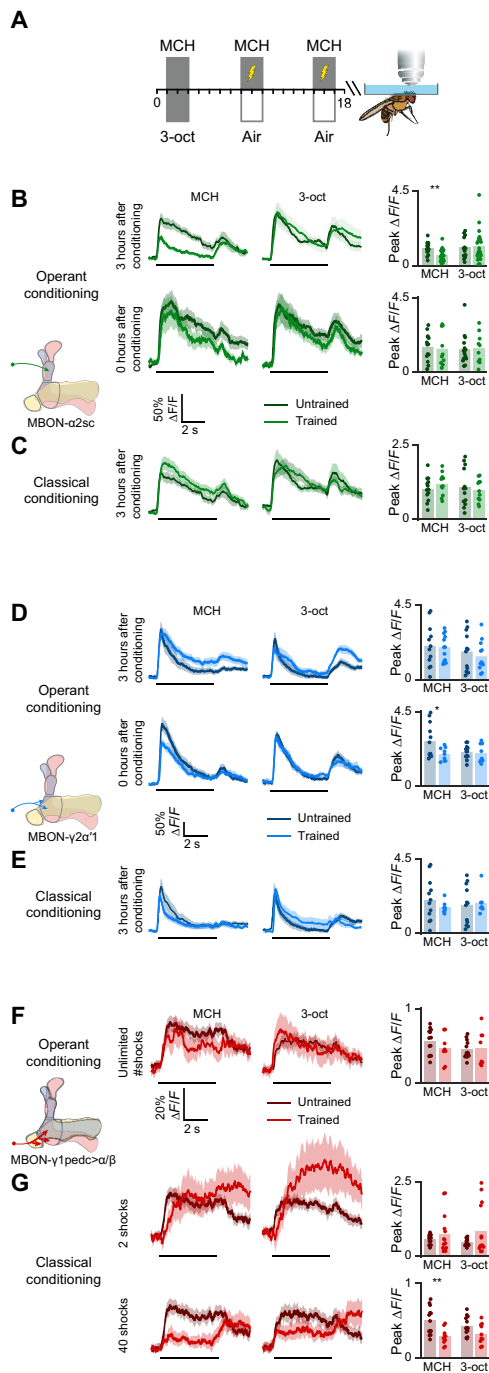


**Fig. 4. Plasticity in MBON response following operant conditioning.** (A) Experimental protocol. Flies were trained (CS<sup>+</sup>-MCH, CS<sup>-</sup>-3-oct), placed in a vial, and neuronal activity was imaged after a specified period using two-photon microscopy. ( $\Delta F/F$  Ca<sup>2+</sup> transients displayed below). (B) Left,  $\alpha 2sc$ -MBON response to CS<sup>+</sup> and CS<sup>-</sup> 3 hours after operant conditioning (trained,  $N = 22$ ; untrained,  $N = 13$ ) or 15 min (trained,  $N = 10$ ; untrained,  $N = 14$ ) after conditioning. Right, peak  $\Delta F/F$ . A significant decrease in CS<sup>+</sup> response was observed only 3 hours after conditioning. (C) Left,  $\alpha 2sc$ -MBON response to the CS<sup>+</sup> and CS<sup>-</sup> 3 hours after classical conditioning [trained,  $N = 11$ ; untrained,  $N = 13$ , the same as (B), top]. Right, peak  $\Delta F/F$ . No significant change in CS<sup>+</sup> response was observed. (D) Left,  $\gamma 2\alpha'1$ -MBON response to CS<sup>+</sup> and CS<sup>-</sup> 3 hours (trained,  $N = 12$ ; untrained,  $N = 12$ ) or 15 min (trained,  $N = 9$ ; untrained,  $N = 12$ ) after operant conditioning. Right, peak  $\Delta F/F$ . A significant decrease in CS<sup>+</sup> response was observed only 15 min after conditioning. (E) Left,  $\gamma 2\alpha'1$ -MBON response to CS<sup>+</sup> and CS<sup>-</sup> [trained,  $N = 7$ ; untrained,  $N = 12$ , the same as (D), top] 3 hours after classical conditioning. Right, peak  $\Delta F/F$ . No significant change in CS<sup>+</sup> response was observed. (F) Left,  $\gamma 1pedc>\alpha/\beta$ -MBON response to CS<sup>+</sup> and CS<sup>-</sup> 3 hours after operant conditioning (trained,  $N = 8$ ; untrained,  $N = 13$ ) with unlimited shocks. Right, peak  $\Delta F/F$ . No significant change in CS<sup>+</sup> response was observed. (G) Left,  $\gamma 1pedc>\alpha/\beta$ -MBON response to CS<sup>+</sup> the CS<sup>-</sup> 3 hours after classical conditioning. 1 [trained,  $N = 14$ ; untrained,  $N = 13$ , the same as (F)] or 20 [trained,  $N = 10$ , untrained,  $N = 13$ , the same as (F)] shocks were paired with the CS<sup>+</sup> in each of the two training sessions. Right, peak  $\Delta F/F$ . A significant decrease in CS<sup>+</sup> response was observed only with 40 shocks. For all panels: dots, single flies; shaded regions, SEM; black scale bar, 5-s odor pulse. \* $P < 0.05$ , \*\* $P < 0.01$ . See table S1 for statistical analysis.

conditioning, we observed a reduction in the odor response to the CS<sup>+</sup> but not to the CS<sup>-</sup> (Fig. 4G). When performing classical conditioning with only two presentations of the US, which did not result in learning (Fig. 1D), we did not observe a change in odor responses (Fig. 4G). Unexpectedly, following operant conditioning, despite the coincidence of the odor and electric shock, we did not observe reduced CS<sup>+</sup> odor response in the classical conditioning pathway (Fig. 4F). We did not observe any plasticity in odor responses when no odors or shocks were used during the training protocol (fig. S10). These results indicate that the formation of operant memories relies on a parallel neural circuit in the learning and memory center of the fly's brain and suggest that active mechanisms exist to prevent plasticity in the neural circuit of classical conditioning during operant conditioning.

### The classical and operant learning pathways interfere with one another

The above results indicate that plasticity does not occur concurrently at the pathways underlying classical and operant conditioning. In addition, operant and classical conditioning result in different, and conflicting, behavioral responses to the CS<sup>+</sup> (Fig. 1, F to H). It is therefore possible that the existence of the two memory traces at the same time may be disadvantageous. To examine this option, we trained flies with either classical or operant conditioning, thus forming electric shock induced LTD in MBONs mediating classical ( $\gamma 1pedc>\alpha/\beta$ -MBON) or operant ( $\alpha 2sc$ - or  $\gamma 2\alpha'1$ -MBON) conditioning, respectively. However, in the retrieval phase, we optogenetically silenced MBON activity belonging to the parallel pathway using *UAS-GtACR2* only when flies entered the part of the chamber that contained the CS<sup>+</sup> (Fig. 5, A to C). Thus, when flies underwent operant conditioning, an artificial memory trace was also generated in the  $\gamma 1pedc>\alpha/\beta$ -MBON only for the CS<sup>+</sup> (Fig. 5, B and C) and vice versa. Silencing the  $\gamma 1pedc>\alpha/\beta$ -MBON CS<sup>+</sup> odor response during the retrieval phase (thus generating an artificial classical memory trace) after operant conditioning, resulted in a significant reduction in behavioral performance (Fig. 5B). This is although silencing the  $\gamma 1pedc>\alpha/\beta$ -MBON during the retrieval phase for both odors, i.e., CS<sup>+</sup> and CS<sup>-</sup>, did not affect operant learning (fig. S4E). Similarly, when we induced during the retrieval phase CS<sup>+</sup>-specific artificial memory trace in the response of the  $\alpha 2sc$ -MBON or the  $\gamma 2\alpha'1$ -MBON after classical training, flies displayed reduced learning performance (Fig. 5C). To verify that the optogenetic manipulation could indeed induce sufficient artificial memory traces and "write" specific memories, we repeated this protocol but for the CS<sup>-</sup>, thus generating an artificial memory trace for the CS<sup>-</sup>. If the artificially induced memory trace is strong enough, this manipulation should assign a negative valence to the CS<sup>-</sup>. In both cases, although MCH was paired with electrical shocks, artificially depressing the response for 3-oct (CS<sup>-</sup>) resulted in an attractive response toward MCH (fig. S11, A and B). We further verified that even without conditioning,  $\alpha 2sc$ -MBON,  $\gamma 2\alpha'1$ -MBON, and  $\gamma 1pedc>\alpha/\beta$ -MBON drive odor attraction as was previously reported (36, 67, 97–100). To this end, we either inhibited or activated each of these MBONs in untrained flies only when the flies entered the part of the chamber containing the odor MCH (fig. S11, C and D). Activation of each of these neurons resulted in attraction to MCH, whereas inhibition of these neurons resulted in aversion from MCH (fig. S11, C and D). Last, we performed classical conditioning against MCH and then further optogenetically inhibited

$\gamma 1pedc>\alpha/\beta$ -MBON when flies entered the MCH odor plume. This manipulation is expected to generate an even stronger memory trace than the physiological LTD memory trace and thus a stronger learning phenotype, as indeed occurred (fig. S11E). Thus, the optogenetic manipulations are all in agreement with the role of these MBONs as driving attraction. Furthermore, when the optogenetic manipulation is at the same pathway that underwent physiological plasticity, an additive effect is observed as expected. Nevertheless, counterintuitively, when the optogenetic manipulation is not at the same pathway that underwent physiological plasticity, interference between the two pathways occurs. Together, these results indicate that the operant and classical learning pathways interfere with one another.

We then sought to examine whether generating the two memory traces in the operant and classical pathways under more natural conditions will have the same effect as the artificial memory traces generated above. To this end, we trained flies in both the classical and operant learning tasks in the same session in a sequential manner (Fig. 5D). When flies were trained in the operant paradigm followed by the classical paradigm, or vice versa, the flies were unable to form an aversive association to the CS<sup>+</sup> (Fig. 5D). This was not because each session consisted of only one training session per learning type as a single training session formed robust learning (Fig. 5D). Above, we have generated memory traces (a physiological one and an artificial one) in both classical and operant pathways. However, it is possible that the dual sequential training resulted in no memory traces altogether and thus no observed CS<sup>+</sup> avoidance. To test how the dual training paradigm affects MBON plasticity, we imaged the  $\alpha 2sc$ -MBON,  $\gamma 2\alpha'1$ -MBON, and  $\gamma 1pedc>\alpha/\beta$ -MBON odor responses following dual training (Fig. 5E). For this experiment, the flies underwent first operant conditioning followed by classical conditioning. Under these conditions, all three MBON types showed a memory trace manifested by LTD for the CS<sup>+</sup> odor responses (Fig. 5, F to H). Thus, as indicated above, concurrent plasticity in both classical and operant neuronal pathways disrupts behavioral performance.

The cumulative results show that under normal conditions, LTD memory traces are not formed in both classical and operant pathways, although the conditions to generate them exist. Furthermore, the formation of both memory traces reveals interference between the two memory pathways and results in no aversion to the reinforced cue. This suggests that classical and operant memories compete for formation. These memories can coexist if formed sequentially, but, in such a case, they cannot be retrieved properly at the behavioral level.

### The serotonergic DPM neuron is involved in operant learning

Previous studies have reported the involvement of the serotonergic system in nonolfactory operant learning, but the underlying neurons were not found (22, 23). The dorsal paired medial (DPM) neuron is a serotonergic neuron that innervates the MB (101). Therefore, we examined whether the DPM neuron is involved in operant learning. Consistent with previous reports showing that the DPM neuron is only involved in long-term classical learning (73, 101–104), optogenetic silencing of DPM activity (Fig. 6A) did not affect short-term classical conditioning (Fig. 6B). Silencing DPM activity completely abolished operant learning performance (Fig. 6C). Similar results were obtained when thermogenetic silencing

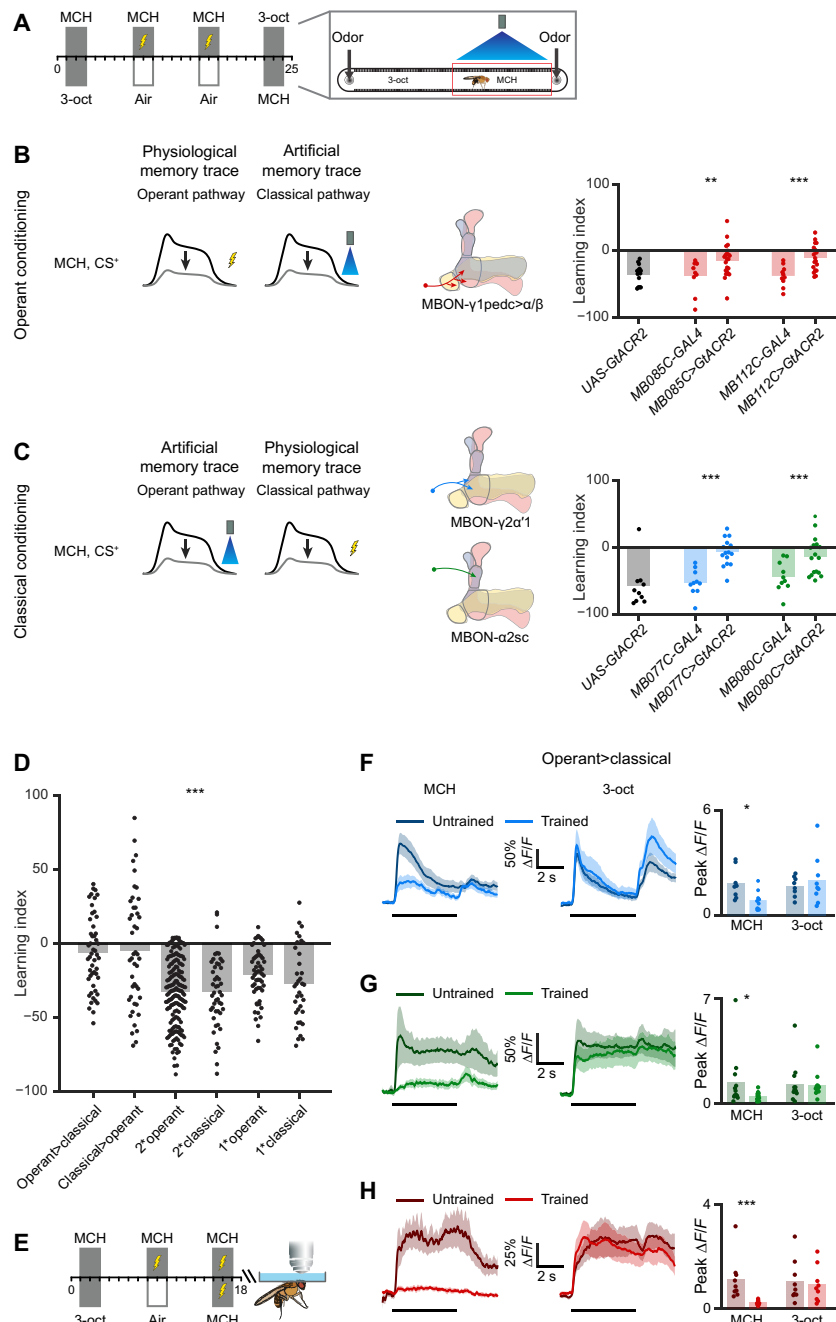


**Fig. 5. Interference between operant and classical learning neuronal circuits.** (A) Experimental protocol. Flies underwent operant or classical conditioning. During the retrieval phase, optogenetic inhibition was activated only when the fly encountered the CS<sup>+</sup>. (B) Silencing the  $\gamma 1pedc>\alpha/\beta$ -MBON (classical pathway) during the retrieval phase after operant training (*UAS-GtACR2*,  $N = 15$ ; *MB085C-GAL4*,  $N = 10$ ; *MB085C-GAL4;UAS-GtACR2*,  $N = 22$ ; *MB112C-GAL4*,  $N = 10$ ; *MB112C-GAL4;UAS-GtACR2*,  $N = 18$ ) significantly decreased learning performance. (C) Silencing the  $\gamma 2\alpha'1$ -MBON (*UAS-GtACR2*,  $N = 10$ ; *MB077C-GAL4*,  $N = 10$ ; *MB077C-GAL4;UAS-GtACR2*,  $N = 15$ ) or the  $\alpha 2sc$ -MBON (*MB080C-GAL4*,  $N = 10$ ; *MB080C-GAL4;UAS-GtACR2*,  $N = 17$ ) during the retrieval phase after classical training significantly decreased learning performance. (D) Flies that underwent operant conditioning followed by classical conditioning, ( $N = 50$ ) or vice versa ( $N = 45$ ), did not display learning. Flies trained in two operant ( $N = 186$ , the same as in Fig. 1B), two classical ( $N = 47$ ) sessions, one operant ( $N = 54$ ), or one classical ( $N = 36$ ) session displayed learning. (E) Experimental protocol. Flies underwent operant conditioning followed by classical conditioning (CS<sup>+</sup>-MCH, CS<sup>-</sup>-3-oct), placed in a new vial, and neuronal activity was imaged using a two-photon microscope following the specified period. (F) Left,  $\gamma 2\alpha'1$ -MBON  $\text{Ca}^{2+}$  response to CS<sup>+</sup> and CS<sup>-</sup> (trained,  $N = 9$ ; untrained,  $N = 8$ ) 15 min after operant conditioning followed by classical conditioning. Right, peak  $\Delta F/F$ . A significant decrease in CS<sup>+</sup> response was observed. (G) Left,  $\alpha 2sc$ -MBON  $\text{Ca}^{2+}$  response to CS<sup>+</sup> and CS<sup>-</sup> (trained,  $N = 12$ ; untrained,  $N = 12$ ) 3 hours after operant conditioning followed by classical conditioning. Right, peak  $\Delta F/F$ . A significant decrease in CS<sup>+</sup> response was observed. (H) Left,  $\gamma 1pedc>\alpha/\beta$ -MBON  $\text{Ca}^{2+}$  response to CS<sup>+</sup> and CS<sup>-</sup> (trained,  $N = 9$ ; untrained,  $N = 9$ ) 3 hours after operant conditioning followed by classical conditioning. Right, peak  $\Delta F/F$ . A significant decrease in CS<sup>+</sup> response was observed. For all panels: dots, single flies; shaded regions, SEM; black scale bar, 5-s odor pulse. \* $P < 0.05$ , \*\* $P < 0.01$ , \*\*\* $P < 0.001$ ; for detailed statistical analysis, see table S1.

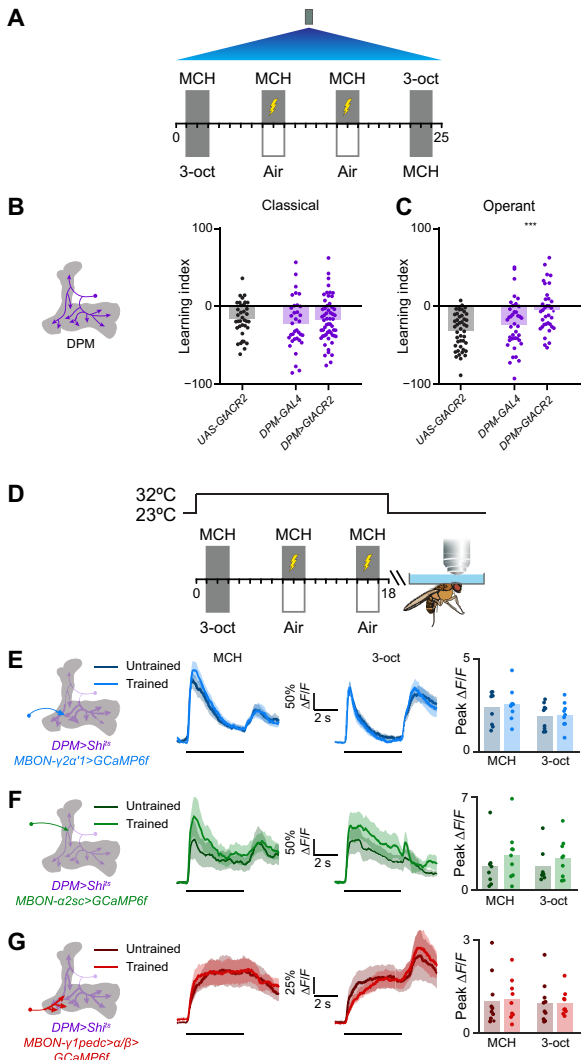


**Fig. 6. DPM involvement in operant learning.** (A) Experimental protocol. Flies underwent operant conditioning, and blue light was shone throughout the entire duration of the experiment to block neuronal activity. (B and C) Optogenetically silencing the DPM neuron using GtACR2 did not affect classical learning (B) (*UAS-GtACR2*,  $N = 36$ ; *DPM-GAL4*,  $N = 35$ ; *DPM-GAL4;UAS-GtACR2*,  $N = 56$ ) but significantly reduced operant learning (C) performance (*UAS-GtACR2*,  $N = 45$ ; *DPM-GAL4*,  $N = 40$ ; *DPM-GAL4;UAS-GtACR2*,  $N = 36$ ). (D) Experimental protocol. Flies underwent operant conditioning followed by classical conditioning ( $CS^+$ -MCH,  $CS^-$ -3-oct), placed in a new vial, and neuronal activity was imaged using a two-photon microscope following the specified period. (E) Left,  $\gamma 2\alpha'1$ -MBON response to  $CS^+$  and  $CS^-$  for trained ( $N = 9$ ) and untrained ( $N = 9$ ) flies in the operant learning paradigm, 15 min after the training paradigm with blocked synaptic release from DPM. *DPM-LexA* and *LexAop-Sh<sup>t51</sup>* were used to block DPM and *MB077C-GAL4* was used to drive *UAS-GCaMP6f*. Right, peak  $\Delta F/F$ . No significant change in  $CS^+$  odor response was observed. (F) Left,  $\alpha 2c$ -MBON response to  $CS^+$  and  $CS^-$  for trained ( $N = 9$ ) and untrained ( $N = 8$ ) flies in the operant learning paradigm, 3 hours after the training paradigm with blocked synaptic release from DPM. *DPM-LexA* and *LexAop-Sh<sup>t51</sup>* were used to block DPM, and *MB080C-GAL4* was used to drive *UAS-GCaMP6f*. Right, peak  $\Delta F/F$ . No significant change in  $CS^+$  odor response was observed. (G) Left,  $\gamma 1pedc>\alpha/\beta$ -MBON response to  $CS^+$  MCH and  $CS^-$  for trained ( $N = 9$ ) and untrained ( $N = 10$ ) flies in the operant learning paradigm, 3 hours after the training paradigm with blocked synaptic release from DPM. *DPM-LexA* and *LexAop-Sh<sup>t51</sup>* were used to block DPM, and *MB085C-GAL4* was used to drive *UAS-GCaMP6f*. Right, peak  $\Delta F/F$ . No significant change in  $CS^+$  odor response was observed. For all panels: dots, single flies; shaded regions, SEM; black scale bar, 5-s odor pulse. \*\*\* $P < 0.001$ ; for detailed statistical analysis, see table S1.

rather the optogenetic silencing was performed (fig. S12A). In addition, silencing DPM either during the training or retrieval phases abolished operant learning (fig. S12, B to E). The above results (Fig. 5) suggest that classical and operant memories compete for formation. Since the DPM neuron shares monosynaptic reciprocal connections with the  $\alpha 2sc$ -MBON,  $\gamma 2\alpha'1$ -MBON, and  $\gamma 1pedc>\alpha/\beta$ -MBON (105), we hypothesized that it might play a role in gating the differential synaptic plasticity and competition that was observed following operant and classical conditioning (Fig. 5). Under this model, DPM activity is required for operant learning and actively prevents LTD in the classical learning pathway. Thus, if this model is correct, blocking DPM activity should prevent operant conditioning-induced LTD in the operant pathway and allow for LTD in the classical pathway. Blocking synaptic release from the DPM neuron abolished the synaptic depression in  $\alpha 2sc$ -MBON and  $\gamma 2\alpha'1$ -MBON following operant learning (Fig. 6, D to F). However, blocking synaptic release from the DPM neuron did not affect  $\gamma 1pedc>\alpha/\beta$ -MBON activity following operant learning (Fig. 6G). Thus, although DPM neuron activity is necessary for the formation of operant memories and the formation of LTD in  $\alpha 2sc$ - and  $\gamma 2\alpha'1$ -MBONs, it does not serve as the gating mechanism between the two forms of memory, i.e., operant and classical memories.

### EPG neurons undergo plasticity following operant conditioning

Different elements of the CX neuronal circuit were previously shown to undergo plasticity following the display of visual external cues (77, 88, 106). As we have found that CX activity is required for operant conditioning, we wanted to test whether CX activity is affected by operant conditioning. Two-photon functional imaging (Fig. 7A) of PEN neurons activity did not display any changes following operant conditioning (Fig. 7B). The same was the case for PFNv neurons (Fig. 7C). However, imaging EPG dendrites in the ellipsoid body revealed an increase in the odor response only for the  $CS^+$  (Fig. 7D). An increase in  $CS^+$  odor response was also observed in flies that underwent classical conditioning; however, it was not significant (Fig. 7E). These results indicate that following learning, EPG neurons receive stronger olfactory inputs or undergo plasticity but only for the  $CS^+$ . EPG axons tile the protocerebral bridge (PB) in a manner in which each heading direction is represented by a particular anatomical location on the PB (89, 92, 107), thus allowing imaging of the EPG population with a greater spatial resolution. Training flies in the operant-conditioning task, where the conditioned odor was presented in the left side of the chamber, caused an increase in both  $CS^+$  and  $CS^-$  odor responses only in the left side of the PB (Fig. 7F). When the conditioned odor was presented in the right side of the chamber, we observed an increase in  $CS^+$  odor response only in the right side of the PB (Fig. 7G) and an increase in  $CS^-$  odor response in the left side of the PB (Fig. 7G). When all light sources were blocked and positional cues were unavailable,  $CS^+$ -specific plasticity was detected on both sides of the PB (fig. S13, A and B). Following classical conditioning, no plasticity was observed in the PB (fig. S13, C and D). Furthermore, no plasticity was observed when no odor or shock was provided during the training phase (fig. S14). These results indicate that only following operant conditioning, odor representation of EPG neurons in PB undergoes plasticity. Furthermore, the anatomical location of this plasticity in the PB was only correlated to the spatial location of the US- $CS^+$ .

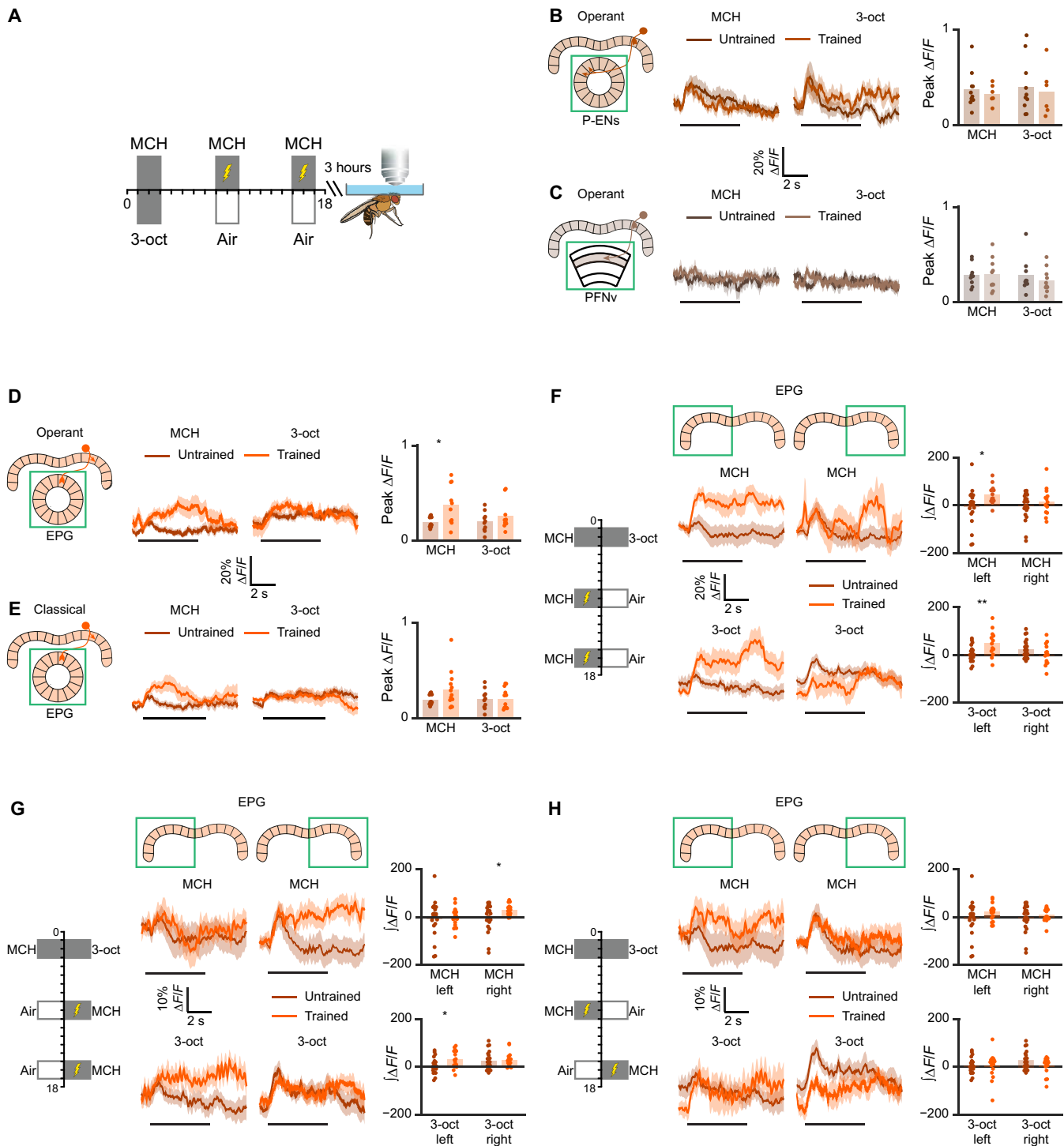


**Fig. 7. CX plasticity following operant training.** (A) Experimental protocol. Flies underwent operant conditioning ( $\text{CS}^+$ -MCH,  $\text{CS}^-$ -3-oct), placed in a vial, and neuronal activity was imaged using a two-photon microscope after 3 hours. (B and C) Left, odor response to  $\text{CS}^+$  and  $\text{CS}^-$  (P-EN neurons: trained,  $N = 6$ ; untrained,  $N = 10$ ; PFNV neurons: trained,  $N = 10$ ; untrained,  $N = 9$ ) following operant conditioning. Right, peak  $\Delta F/F$ . No significant change in  $\text{CS}^+$  response was observed. (D and E) Left, EPG neurons response in the ellipsoid body to  $\text{CS}^+$  and  $\text{CS}^-$  [operant conditioning: trained,  $N = 10$ ; untrained,  $N = 10$ ; classical conditioning; trained,  $N = 13$ ; untrained,  $N = 10$ , the same as (D)]. Right, peak  $\Delta F/F$ . A significant increase in  $\text{CS}^+$  response was observed only following operant conditioning. (F to H) EPG neuron responses in the left and right PB to  $\text{CS}^+$  and  $\text{CS}^-$ . (F)  $\text{CS}^+$  was presented on the left (trained,  $N = 13$ ; untrained,  $N = 22$ ), showing a significant increase in  $\text{CS}^+$  response in the left PB, correlated with the chamber side where  $\text{CS}^+$  was coupled to the US, and a significant increase in  $\text{CS}^-$  response in the left PB. (G)  $\text{CS}^+$  was presented on the right [trained,  $N = 16$ ; untrained,  $N = 22$ , the same as (F)], with a significant change in  $\text{CS}^+$  response in the right PB, correlated with the  $\text{CS}^+$  side, and a significant increase in  $\text{CS}^-$  response in the left PB, unrelated to US presentation. (H)  $\text{CS}^+$  was alternated between left and right across sessions [trained,  $N = 16$ ; untrained,  $N = 22$ , the same as (F)] with no significant changes in odor response observed. For all panels: dots, single flies; shaded regions, SEM; black scale bar, 5-s odor pulse. \* $P < 0.05$ , \*\* $P < 0.01$ ; for detailed statistical analysis, see table S1.

pairing. The observed plasticity for the CS<sup>-</sup> was irrespective of the US location and thus not related to the CS-US pairing.

CX activity can contribute to the formation of operant memories in two ways. First, it could facilitate the formation of the memory at the acquisition stage. Second, it could facilitate the avoidance of the CS<sup>+</sup> during the retrieval phase. Optogenetically silencing CX activity using *SS00096-GAL4*, which drives expression in EPG neurons and *UAS-GtACR2* during acquisition or retrieval, eliminated the operant memory, indicating that CX activity is required in both phases (fig. S8, K and L). We then sought to examine whether the observed CX plasticity that was correlated with the spatial location of the US-CS<sup>+</sup> pairing was relevant during the retrieval phase. To this end, we alternated the location of the CS<sup>+</sup> in the chamber from left to right during the same training session (Fig. 7H). Following this training protocol, we did not observe any plasticity in the PB (Fig. 7H), indicating that CX plasticity is not necessary for operant memory retrieval as flies were able to form operant memories in this training protocol (fig. S1B). These results suggest that the specific US-CS<sup>+</sup>-induced CX plasticity is required during the acquisition phase, and overall CX activity is required throughout the operant conditioning process.

### EPG activity gates MBON plasticity during operant learning

Since CX activity is required for operant conditioning, we hypothesized that it might play a role in gating the differential MBON synaptic plasticity that indicated the competition between the formation of operant and classical conditioning (Fig. 5). As mentioned above, under this model, CX activity is required for operant learning and actively prevents LTD in the classical learning pathway. Thus, if this model is correct, blocking CX activity should prevent operant conditioning-induced LTD in the operant pathway and allow for LTD in the classical pathway. To test this hypothesis, we blocked synaptic release from EPG neurons using *EPG-LexA* and *LexAop-Shi<sup>ts1</sup>* and imaged the activity of the operant conditioning-related neurons,  $\alpha 2sc$ - and  $\gamma 2\alpha'1$ -MBONs and of the classical conditioning-related neuron  $\gamma 1pedc>\alpha/\beta$ -MBON after operant conditioning (Fig. 8A). Consistent with our hypothesis, the operant-conditioning MBONs,  $\alpha 2sc$ - and  $\gamma 2\alpha'1$ -MBONs, showed no LTD to the CS<sup>+</sup> (Fig. 8, B and C). Furthermore, when we blocked synaptic release from the CX during operant training and imaged the  $\gamma 1pedc>\alpha/\beta$ -MBON odor response, we did observe LTD for the CS<sup>+</sup> (Fig. 8D). As explained above, the flies are conditioned in the behavior apparatus and then transferred to the two-photon microscope to perform functional imaging (Fig. 8A). Blocking CX synaptic release was only performed at the behavior apparatus where memory acquisition occurred and not under the two-photon microscope where memory retrieval was performed. Thus, CX activity gates plasticity at the two memory pathways during the acquisition of operant memories. Together, under normal conditions, CX activity is necessary to enable synaptic plasticity in the operant learning pathway and prevent synaptic plasticity in the classical learning pathway during operant learning.

### DISCUSSION

Here, we elucidate the neuronal circuit underlying aversive olfactory operant learning in *Drosophila* (Fig. 9). Our findings reveal how flies learn through active engagement with their environment, contrasting it with the more passive nature of classical conditioning. We

demonstrate that operant and classical learning rely on parallel MB neuronal pathways. We show that flies execute different behaviors when presented with the CS following operant and classical learning. More so, we show that contrary to the current dogma, operant and classical learning memories cannot be formed simultaneously and that both artificial optogenetic memory induction and behavioral training of both pathways abolished learning. We also show a role for the CX in operant learning. We find that it undergoes plasticity following operant conditioning and that it gates MBON synaptic plasticity, which separates the operant and classical learning pathways.

A key unanswered question in the fields of classical and operant learning is the way the two processes interact. This is because the initial encounters with the paired US and CS<sup>+</sup> are identical in operant and classical learning (until an association is formed between the operant action and the US and CS<sup>+</sup>). According to the current dogma, a classical memory is formed, which is later followed by an operant memory (6). Furthermore, according to this view, classical and operant memories are additive and work in concert (108, 109). This is despite the fact that classical and operant memories can lead to different behavioral outputs and that operant memories can form under conditions that do not generate classical memories (1, 4, 8–10). We show that *Drosophila* shares the same principles of learning with the mammalian system. Like the mammalian system, classical and operant memories are formed in parallel neuronal pathways. Furthermore, as in the mammalian system, these two different memories can drive different behavioral outputs. The superb genetic toolkit available for flies allowed us to resolve the above problem where two memories driving different behaviors are supposedly formed. We show that contrary to the current dogma, there are active processes that are used when operant conditioning takes place and that prevent classical memory simultaneous co-formation. In this context, recently, it was demonstrated that during decision-making, choices activate neurons that suppress the neural pathways of other decision options (110). Thus, it seems that a similar strategy is used for the formation of memories and for the execution of decisions.

The present study unveils behavioral distinctions following operant and classical aversive olfactory learning in *Drosophila*, potentially reflecting divergent cognitive processes between these learning forms. This finding aligns with observations in mammals and humans, where active and passive avoidance strategies represent distinct cognitive approaches (8, 9). This constitutes a different conceptual framework within the realm of aversive olfactory learning in *Drosophila*. Traditionally, studies exclusively assess the preference for the CS<sup>+</sup> relative to the CS<sup>-</sup>. Consequently, the isolated response to the CS<sup>+</sup> remains largely unexplored. Our work underscores the importance of implementing diverse behavioral assays, as evidenced by the uncovering of previously overlooked outcomes. The observed behavioral divergence between operant and classically conditioned flies suggests potentially profound differences in cognitive engagement. Operant learning, inherently active, may involve complex decision-making and flexible responses. In contrast, classical conditioning might rely on more passive, stimulus-driven associations. By venturing beyond conventional preference tests, we illuminate a pathway toward comprehending the rich spectrum of learning strategies used by *Drosophila*.

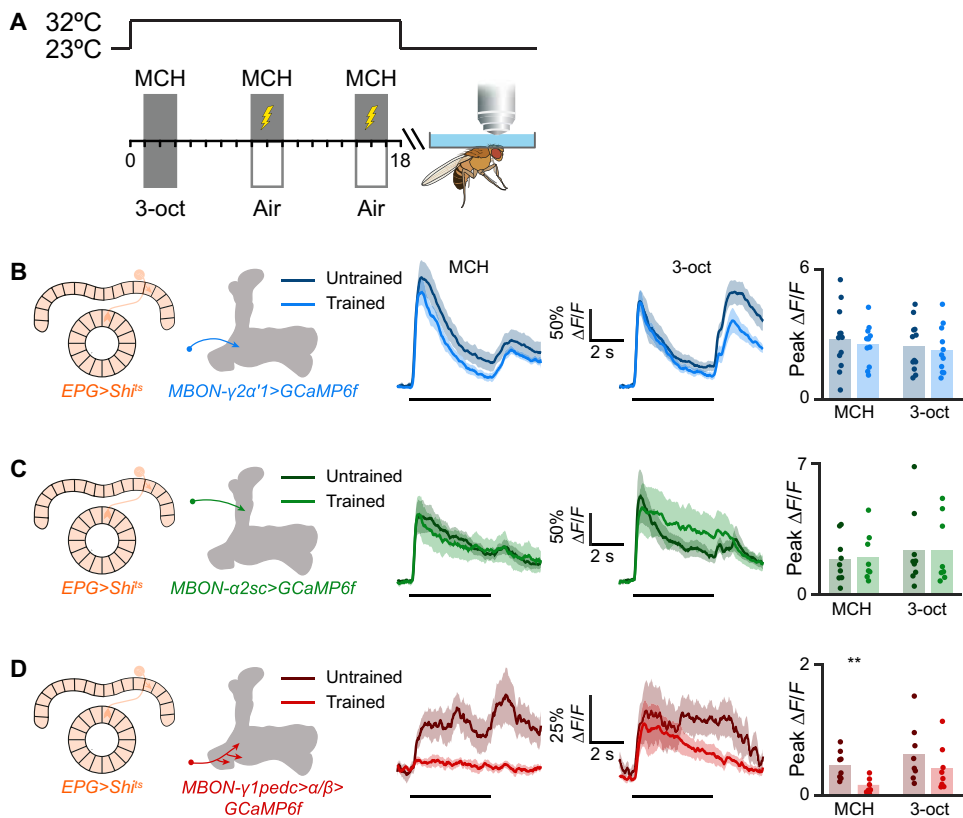


**Fig. 8. CX activity gates  $\gamma 1pedc > \alpha/\beta$ -MBON plasticity.** (A) Experimental protocol. Flies were trained in the behavioral apparatus and were then placed in a new vial for the specified period of time. Following this time period, neuronal activity was imaged using a two-photon microscope. (B) Left,  $\Delta F/F$  odor induced  $\text{Ca}^{2+}$  transient measured in  $\gamma 2\alpha' 1$ -MBON in response to the CS<sup>+</sup> (MCH) and the CS<sup>-</sup> (3-oct) for trained ( $N = 11$ ) and untrained ( $N = 12$ ) flies in the operant learning paradigm 15 min after the training paradigm with blocked synaptic release from CX. *EPG-LexA* and *LexAop-Shi<sup>ts1</sup>* were used to block CX, and *MB077C-GAL4* was used to drive *UAS-GCaMP6f*. Right, peak response of the left presented traces. No significant change in CS<sup>+</sup> odor response was observed. (C) Left,  $\Delta F/F$  odor induced  $\text{Ca}^{2+}$  transient measured in  $\alpha 2sc$ -MBON in response to the CS<sup>+</sup> (MCH) and the CS<sup>-</sup> (3-oct) for trained ( $N = 8$ ) and untrained ( $N = 9$ ) flies in the operant learning paradigm 3 hours after the training paradigm with blocked synaptic release from CX. *EPG-LexA* and *LexAop-Shi<sup>ts1</sup>* were used to block CX, and *MB080C-GAL4* was used to drive *UAS-GCaMP6f*. Right, peak response of the left presented traces. No significant change in CS<sup>+</sup> odor response was observed. (D) Left,  $\Delta F/F$  odor induced  $\text{Ca}^{2+}$  transient measured in  $\gamma 1pedc > \alpha/\beta$ -MBON in response to the CS<sup>+</sup> (MCH) and the CS<sup>-</sup> (3-oct) for trained ( $N = 8$ ) and untrained ( $N = 8$ ) flies in the operant learning paradigm 3 hours after the training paradigm with blocked synaptic release from CX. *EPG-LexA* and *LexAop-Shi<sup>ts1</sup>* were used to block CX, and *MB085C-GAL4* was used to drive *UAS-GCaMP6f*. Right, peak response of the left presented traces. A significant decrease in CS<sup>+</sup> odor response was observed. For all panels, dots represent single flies. Shaded regions represent SEM. Black scale bar, 5-s odor pulse. \*\* $P < 0.01$ ; for detailed statistical analysis, see table S1.

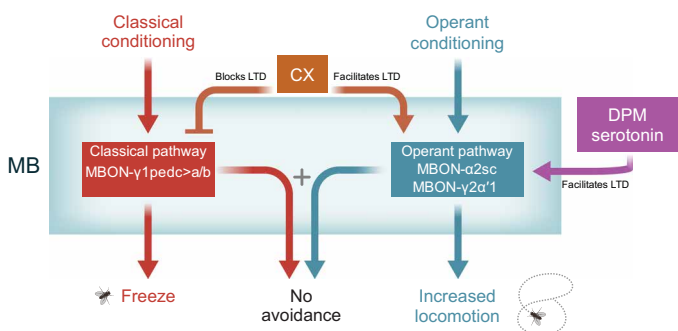


**Fig. 9. Model for the interaction between operant and classical learning.** Operant conditioning requires  $\gamma 2\alpha' 1$ - and  $\alpha 2sc$ -MBON that show CS<sup>+</sup>-specific LTD following operant conditioning and results in an active avoidance response. For operant conditioning, DPM and EPG activity is required. Classical conditioning requires  $\gamma 1pedc > \alpha/\beta$ -MBON, which show CS<sup>+</sup>-specific LTD following classical conditioning and results in a passive avoidance response. Classical conditioning does not require DPM activity, but LTD in this pathway is suppressed following EPG neurons activity. The occurrence of LTD in both operant and classical pathways results in no avoidance response.

In this work, we show that operant and classical learning rely on parallel MBON pathways. However, our results somewhat differ from previously reported finding regarding the roles of specific MBONs in classical learning. For example, we did not observe LTD in the  $\alpha 2sc$ -MBON and  $\gamma 2\alpha' 1$ -MBON following classical learning, as opposed to previous reports (36, 37, 60, 68, 71). This discrepancy may arise from the use of different behavioral paradigms and experimental conditions. Previous studies have shown that different neuronal mechanisms are involved when using a different behavioral apparatus to test the same behavior (111, 112). In addition, the observed MBON LTD could also depend on the experimental conditions. For example, in some cases, LTD can be observed in MBON- $\alpha 2'$  following classical learning (36), and, in other cases, it could not be observed (37). Thus, future studies using different behavioral paradigms for operant learning would help validate the role of specific MBONs in operant learning.

Here, we describe the involvement of different elements of the MB circuit in operant learning. However, the names used to describe each cell type are based on coarse anatomical features, which were given

before a detailed connectome of the fly brain was obtained (26). This can lead to some confusion regarding the interpretation of the results. For example, we find that the neurons covered by the driver line named PPL1- $\gamma$ 1pedc are necessary for operant learning, yet the MBON innervating this region is not required for operant conditioning. However, PPL1- $\gamma$ 1pedc neurons are not restricted to the  $\gamma$ 1 neural compartment of the MB. This driver line covers the SMP. MB\_PED.1 neuron (105, 113) that sends axonal arborizations mostly to the  $\gamma$ 1 compartment. However, it also innervates MBONs belonging to the  $\gamma$ 2,  $\gamma$ 3, and  $\gamma$ 4 compartments and the DPM neuron (105). More so, this neuron also overlaps with  $\alpha/\beta$  KC in the peduncle (26, 114). Thus, it is possible that PPL1- $\gamma$ 1pedc mediates its effect on operant conditioning not via the  $\gamma$ 1 peduncle but rather via other neurons. Another example is the apparent discrepancy between the fact that  $\alpha/\beta$  KC are not necessary for operant learning, while the MBON- $\alpha$ 2sc is necessary for operant learning. Since MBONs are the key output neurons of the MB and serve as an MB hub, they may be more sensitive to perturbations. For instance, the MBON- $\alpha$ 2sc receives inputs from a number of MBONs (MBON- B1>a, MBON-a2sp, MBON-a'2, MBON- $\gamma$ 1pedc>a/B, and MBON-a2sc) and from the modulatory APL and DPM neurons (105). Thus, care should be taken when interpreting the involvement of PPL1- $\gamma$ 1pedc and other neurons in operant learning since their anatomical features are not directly evident from their naming scheme.

Our results demonstrate that activity of EPG neurons is required to promote plasticity in  $\alpha$ 2sc-MBON and  $\gamma$ 2 $\alpha'$ -1-MBON, related to operant conditioning, and to prevent plasticity in  $\gamma$ 1pedc> $\alpha/\beta$ -MBON. Furthermore, we show that EPG activity is required for behavioral output during both acquisition and retrieval. However, blocking EPG activity only at the acquisition stage (Fig. 8, A to D) is sufficient to prevent plasticity of the “operant” MBONs and enable it in the “classical” MBONs. Thus, while EPG activity is required for operant conditioning at both acquisition and retrieval, only the former is involved in MBON plasticity. In addition, while MB connections to the CX were clearly demonstrated (84, 115, 116), the opposite pathway from CX to MB is less clear. How then is information from EPG neurons conveyed back to MB, and, more interestingly, how such information gates neuronal plasticity remains to be found in future studies.

Our discovery of CX plasticity following operant learning and that CX activity gates LTD in the MB classical and operant learning pathways opens exciting avenues for future investigation. Our serendipitous discovery of PB plasticity was a result of an unintentional light source in our behavioral apparatus. This provided a common visual landmark that was able to synchronize neuronal activity in the PB (76, 83, 117), which allowed us to observe PB plasticity in a common anatomical location across different flies. Future studies should investigate the interaction between visual cues, olfactory operant learning, and CX plasticity in greater detail. More so, elucidating the mechanisms underlying CX plasticity in aversive olfactory operant learning is particularly compelling. Prior work highlights dopaminergic involvement in CX plasticity during visual navigation tasks (77, 88, 106). Future studies could explore whether CX plasticity results from direct dopaminergic input and its underlying molecular mechanisms, or if increased CX activity reflects stronger synaptic inputs. Unraveling these mechanisms would pave the way for research on the functional role of CX plasticity in gating LTD in MBONs. While our data suggest its importance during training, since it is only detectable if the CS<sup>+</sup> and US are presented in the same

place in both training sessions, further work is needed to confirm and define its precise role. These lines of inquiry, although beyond this study’s scope, hold substantial promise for understanding the interplay between the operant and classical learning systems.

The findings of this study represent a major step forward in understanding operant conditioning in *Drosophila* but, more importantly, address the general open question of the relation between classical and operant conditioning. Thus, this study paves the way for future investigations in flies into various aspects of the complex behavior of operant conditioning, including reward processing, decision-making, and the potential for higher-order cognitive functions that can be used to understand the relation between classical and operant conditioning in the more sophisticated mammalian system.

## MATERIALS AND METHODS

### Fly strains

Fly strains (see below) were raised on cornmeal agar under a 12-hour light/12-hour dark cycle at 25°C. For activation of CsChrimson or GtACR2, the flies were collected immediately after eclosion and grown for another 3 to 5 days on 1 mM all-trans retinal (R2500; Sigma-Aldrich) supplemented food in complete darkness before experimental testing was performed. The following fly strains were used: *w[1118]* (BDSC\_5905), *UAS-shi[ts1]* (BDSC\_66600), *GAL4-OK107* (BDSC\_854), *GAL4-c305a* (BDSC\_30829), *GAL4-MB247* (BDSC\_50742), *GAL4-MB504B* (BDSC\_68329), *GAL4-MB320C* (BDSC\_68253), *GAL4-MB438B* (BDSC\_68326), *GAL4-MB077C* (BDSC\_68284), *GAL4-MB080C* (BDSC\_68285), *GAL4-SS00090* (BDSC\_75849), *GAL4-SS00096* (BDSC\_86861), *GAL4-GMR37F06* (BDSC\_49962), *GAL4-SS52628* (BDSC\_76008), *GAL4-SS00078* (BDSC\_75854), *UAS-GCaMP6f* (BDSC\_42747), *GAL4-MB085C* (BDSC\_68288), *UAS-GtACR2* (BDSC\_92984), *UAS-CsChrimson* (BDSC\_55135), *GAL4-MB112C* (BDSC\_68263), *GAL4-DPM* (VTID\_VT64246), *GAL4-71G10* (BDSC\_39604), *GAL4-R28H05* (BDSC\_49472), *GAL4-MB296B* (BDSC\_68308), *GAL4-MB304B* (BDSC\_68367), *GAL4-MB058B* (BDSC\_68278), *GAL4-MB099C* (BDSC\_68290), *GAL4-MB308B* (BDSC\_68312), *GAL4-MB630B* (BDSC\_68334), *GAL4-MB018B* (BDSC\_68296), *GAL4-MB027B* (BDSC\_68301), *GAL4-MB065B* (BDSC\_68281), *GAL4-MB074C* (BDSC\_68282), *GAL4-MB433B* (BDSC\_68324), *GAL4-MB399B* (BDSC\_68369), *GAL4-MB298B* (BDSC\_68309), *GAL4-MB310C* (BDSC\_68313), *GAL4-MB002B* (BDSC\_68305), *GAL4-MB549C* (BDSC\_68373), *GAL4-R58E02* (BDSC\_41347), *UAS-FLPTH-C* (BDSC\_93705), *UAS-(FRT.stop)shi[ts]* (BDSC\_66676), *GAL4-GMR30B10* (BDSC\_49522), *GAL4-GMR46F02* (BDSC\_50273), *DPM-LexA* (gift from Ann-Shyn Chiang), *LexAop-Shi<sup>ts1</sup>* (gift from M. Silies), *EPG-LexA* (BDSC\_52867).

### Olfactory stimulation during two-photon imaging

Odors (the purest level available) were obtained from Sigma-Aldrich (Rehovot, Israel). Odor flow of  $0.4\text{ l}/\text{min}$  ( $10^{-1}$  or  $10^{-2}$  dilution) was combined with a carrier air stream of  $0.4\text{ l}/\text{min}$  using mass-flow controllers (Sensirion) and software-controlled solenoid valves (The Lee Company). This resulted in a final odor dilution of  $5 \times 10^{-1}$  or  $5 \times 10^{-2}$  delivered to the fly. Odor flow was delivered through a 1/16-inch (0.15875 cm) ultrachemical-resistant Versilon polyvinyl chloride tubing (Saint-Gobain, NJ, USA) placed 5 mm from the fly’s antenna.

## Functional imaging

Imaging was carried out as previously described (40, 42, 45) using two-photon laser-scanning microscopy (DF-Scope installed on an Olympus BX51WI microscope). The flies were anesthetized on ice and then moved to a custom-built chamber and fixed to aluminum foil using wax while walking on a Styrofoam ball. Cuticle and trachea were removed from the area of interest, and the exposed brain was superfused with carbonated solution as described above. Odors were delivered at a final dilution of  $5 \times 10^{-2}$ , and fluorescence was excited by a Ti-Sapphire laser (Mai Tai HP DS, 100 fs pulses) centered at 910 nm, attenuated by a Pockels cell (Conoptics) and coupled to a galvo-resonant scanner. Excitation light was focused by a 20 $\times$ , 1.0 numerical aperture objective, and emitted photons were detected by GaAsP photomultiplier tubes (Hamamatsu Photonics, H10770PA-40SEL), whose currents were amplified (Hamamatsu HC-130-INV) and transferred to the imaging computer (MScan 2.3.01). All two-photon imaging experiments were acquired at 30 Hz. For presentation purposes only, imaging data were smoothed using a moving average of five frames. In experiments where imaging was carried out after training, the flies did not undergo the final odor preference test and were removed from the incubator and placed in a new vial. For 0 hours after conditioning experiments, the flies were cold anesthetized and imaged immediately and up to 15 min after training. For 3 hours after conditioning experiments, the flies were cold anesthetized and imaged 3 hours after training. To avoid changes in odor responses due to habituation, each fly was presented with only one trial of the odor in the imaging experiments. Odors were presented in a pseudorandom order to the fly to avoid any order effects in odor responses.

## Behavioral assay

Experiments were performed using a custom-built, fully automated apparatus (14, 40, 118). Single flies were housed in clear chambers (polycarbonate, length, 50 mm; width, 5 mm; height, 1.3 mm). Mass flow controllers (CMOSens PerformanceLine, Sensirion) were used to control air flow. An odor stream (0.3 l/min) obtained by circulating the air flow through vials filled with a liquid odorant was combined with a carrier flow (2.7 l/min). Odors were prepared at  $10^{-1}$  (3-oct) or  $10^{-2}$  (MCH) dilution. Fresh odors were prepared daily.

Two identical odor delivery systems were used, each delivering odors independently to each half of the chamber. The total flow (3 liter/min, carrier and odor stimulus) was split between 20 chambers. The air flow from the two halves of the chamber converged at a central choice zone. The 20 chambers were stacked in two columns each containing 10 chambers and were backlit by 940-nm light-emitting diodes (LEDs) (Vishay TSAL6400) combined with 470- or 590-nm LEDs for optogenetics experiments. Images were obtained by a MAKO complementary metal-oxide semiconductor camera (Allied Vision Technologies) equipped with a Computar M0814-MP2 lens. The apparatus was operated in a temperature-controlled incubator (Panasonic MIR 154) at 25°C. For *shibire*<sup>ts1</sup> experiments, the flies were placed in an incubator set to 32°C for 5 min before the start of the experiment. Unless specified otherwise, for all experiments involving *shibire*<sup>ts1</sup>, the restrictive temperature of 32°C was maintained for the entire duration of the experiment. For Figs. 6 (D and E) and 8, the flies were trained at 32°C and imaging experiments were performed at 23°C.

Fly position was extracted from video images using a virtual instrument written in LabVIEW 7.1 (National Instruments). The same virtual instrument was also used to control odor delivery. Data were analyzed in MATLAB 2018a (The MathWorks).

The classical conditioning protocol included 20 equally spaced 1.25-s electric shocks at 80 V and was repeated twice. The protocol used was adapted to correspond to the operant protocol. It differs from previous published classical protocols (40, 44, 119) in that the CS<sup>-</sup> was not presented alone. We chose this paradigm to avoid the recently found appetitive safety memories attributed to the CS<sup>-</sup> (46, 47) so that our task is strictly aversive in nature. During the classical learning protocol, the flies were initially presented with the CS<sup>+</sup> and CS<sup>-</sup> for 2 min to assess initial odor valence. Following 5 min, two training sessions, 5 min apart were conducted, as mentioned above. Five minutes after the last training session, the flies were presented with the CS<sup>+</sup> and CS<sup>-</sup> for 2 min to assess odor valence and learning. The learning index was calculated as (preference for CS<sup>+</sup> before training)–(preference for CS<sup>+</sup> after training). The operant conditioning protocol (14) used the extracted fly position in the chamber and presented a shock if the fly crossed to the half of the chamber containing the odor. The preference score used in fig. S11 was calculated as (time spent in MCH)/(total time). Freezing events were defined as instances where a fly did not move for more than 1 s. The protocol used in this study differs from the previously published protocol (14) in that during the training session flies have a choice between air and an odor (usually MCH) rather than a choice between two odors (MCH and 3-oct). This is because it was demonstrated that when two odors are used during training, the flies form in addition to an aversive memory to the CS<sup>+</sup>, also a safety memory to the CS<sup>-</sup> (46, 47). Each shock lasted 1.25 s at 80 V and was separated by a minimum period of 0.2 s. The maximal number of shocks was 400 unless otherwise stated. The operant protocol sequence was identical to the classical protocol, with the exception of the nature of the training session. Flies that did not move during the operant training sessions or during the odor preference testing phase as well as flies that did not receive electrical shocks during the training sessions were excluded from the analysis.

## Quantification and statistical analysis

### Statistics and data analysis

All statistical testing and parameter extraction were done using MATLAB (The MathWorks Inc.). All details of statistical tests are given in table S1. Significance was defined as a *P* value smaller than 0.05, and all statistical tests were two-sided. Normality assumption was tested using the Shapiro-Wilk test (<https://mathworks.com/matlabcentral/fileexchange/13964-shapiro-wilk-and-shapiro-francia-normality-tests>). In cases where the normality assumption was violated, a permutation test was used using the “permutationTest” function in MATLAB (<https://github.com/lrkrol/permutationTest>).

Effect size was calculated with the Measures of Effect Size (MES) Toolbox <https://github.com/hhentschke/measures-of-effect-size-toolbox/blob/master/readme.md>). Permutation test was used using the permutationTest function in MATLAB (<https://github.com/lrkrol/permutationTest>). For presentation, bar plots with dots were generated using the UnivarScatter MATLAB ToolBox (<https://mathworks.com/matlabcentral/fileexchange/54243-univarscatter>) and the shadedErrorBar function (<https://github.com/raacampbell/shadedErrorBar>) for shaded errors on imaging traces.

## Supplementary Materials

This PDF file includes:

Figs. S1 to S14

Table S1

## REFERENCES AND NOTES

1. J. Ledoux, N. D. Daw, Surviving threats: Neural circuit and computational implications of a new taxonomy of defensive behaviour. *Nat. Rev. Neurosci.* **19**, 269–282 (2018).
2. F. K. McSweeney, E. S. Murphy, *The Wiley Blackwell Handbook of Operant and Classical Conditioning*. (Wiley-Blackwell, 2014), pp. 1–768.
3. C. Bravo-Rivera, C. Roman-Ortiz, E. Brignoni-Perez, F. Sotres-Bayon, G. J. Quirk, Neural structures mediating expression and extinction of platform-mediated avoidance. *J. Neurosci.* **34**, 9736–9742 (2014).
4. L. Jing, C. Ma, L. Xu, G. Richter-Levin, Distinct neural representations and cognitive behaviors attributable to naturally developed active avoidance or reactive escape Strategies in the male rat. *Int. J. Neuropsychopharmacol.* **26**, 761–772 (2023).
5. G. Lázaro-Muñoz, J. E. LeDoux, C. K. Cain, Sidman instrumental avoidance initially depends on lateral and basal amygdala and is constrained by central amygdala-mediated Pavlovian processes. *Biol. Psychiatry* **67**, 1120–1127 (2010).
6. J. W. Rudy, N. C. Huff, P. Matus-Amat, Understanding contextual fear conditioning: Insights from a two-process model. *Neurosci. Biobehav. Rev.* **28**, 675–685 (2004).
7. C. K. Cain, N. S. Kline, Avoidance problems reconsidered. *Curr. Opin. Behav. Sci.* **26**, 9–17 (2019).
8. R. M. Sears, R. C. R. Martinez, N. Gupta, G. La, S. Kim, J. M. Moscarello, J. E. LeDoux, C. K. Cain, Active vs. reactive threat responding is associated with differential c-Fos expression in specific regions of amygdala and prefrontal cortex. *Learn. Mem.* **20**, 446–452 (2013).
9. J. M. Moscarello, J. E. LeDoux, Active avoidance learning requires prefrontal suppression of amygdala-mediated defensive reactions. *J. Neurosci.* **33**, 3815–3823 (2013).
10. B. Brembs, M. Heisenberg, The operant and the classical in conditioned orientation of *Drosophila melanogaster* at the flight simulator. *Learn. Mem.* **7**, 104–115 (2000).
11. R. L. Davis, Learning and memory using *Drosophila melanogaster*: A focus on advances made in the fifth decade of research. *Genetics* **224**, iyad085 (2023).
12. J. Felsenberg, Changing memories on the fly: The neural circuits of memory re-evaluation in *Drosophila melanogaster*. *Curr. Opin. Neurobiol.* **67**, 190–198 (2021).
13. B. Brembs, Mushroom bodies regulate habit formation in *Drosophila*. *Curr. Biol.* **19**, 1351–1355 (2009).
14. A. Claridge-Chang, R. D. Roorda, E. Vrontou, L. Sjulson, H. Li, J. Hirsh, G. Miesenböck, Writing memories with light-addressable reinforcement circuitry. *Cell* **139**, 405–415 (2009).
15. A. E. Rajagopalan, R. Darshan, K. L. Hibbard, J. E. Fitzgerald, G. C. Turner, Reward expectations direct learning and drive operant matching in *Drosophila*. *Proc. Natl. Acad. Sci. U.S.A.* **120**, e2221415120 (2023).
16. M. Ahmed, A. E. Rajagopalan, Y. Pan, Y. Li, D. L. Williams, E. A. Pedersen, M. Thakral, A. Previero, K. C. Close, C. P. Christoforou, D. Cai, G. C. Turner, E. J. Clowney, Input density tunes Kenyon cell sensory responses in the *Drosophila* mushroom body. *Curr. Biol.* **33**, 2742–2760.e12 (2023).
17. K. Vogt, C. Schnaitmann, K. V. Dylla, S. Knapke, Y. Aso, G. M. Rubin, H. Tanimoto, Shared mushroom body circuits underlie visual and olfactory memories in *Drosophila*. *eLife* **3**, e02395 (2014).
18. A. Ehweiner, C. Duch, B. Brembs, Wings of Change: A PKC/FoxP-dependent plasticity in steering motor neurons underlies operant selflearning in *Drosophila*. bioRxiv 520755 [Preprint] (2023). <https://doi.org/10.1101/2022.12.16.520755>.
19. T. D. Wiggin, Y. Hsiao, J. B. Liu, R. Huber, L. C. Griffith, Rest is required to learn an appetitively-reinforced operant task in *Drosophila*. *Front. Behav. Neurosci.* **15**, 681593 (2021).
20. B. Brembs, W. Plendl, Double dissociation of PKC and AC manipulations on operant and classical learning in *Drosophila*. *Curr. Biol.* **18**, 1168–1171 (2008).
21. N. Nuwal, P. Stock, J. Hiemeyer, B. Schmid, A. Fiala, E. Buchner, Avoidance of heat and attraction to optogenetically induced sugar sensation as operant behavior in adult *Drosophila*. *J. Neurogenet.* **26**, 298–305 (2012).
22. E. C. Croteau-Chonka, M. S. Clayton, L. Venkatasubramanian, S. N. Harris, B. M. W. Jones, L. Narayan, M. Winding, J. B. Masson, M. Zlatic, K. T. Klein, High-throughput automated methods for classical and operant conditioning of *Drosophila* larvae. *eLife* **11**, e70015 (2022).
23. D. Sitaraman, E. F. Kramer, L. Kahsai, D. Ostrowski, T. Zars, Discrete serotonin systems mediate memory enhancement and escape latencies after unpredicted aversive experience in *Drosophila* place memory. *Front. Syst. Neurosci.* **11**, 92 (2017).
24. S. Diegelmann, M. Zars, T. Zars, Genetic dissociation of acquisition and memory strength in the heat-box spatial learning paradigm in *Drosophila*. *Learn. Mem.* **13**, 72–83 (2006).
25. R. Wolf, M. Heisenberg, Basic organization of operant behavior as revealed in *Drosophila* flight orientation. *J. Comp. Physiol. A* **169**, 699–705 (1991).
26. Y. Aso, D. Hattori, Y. Yu, R. M. Johnston, N. A. Iyer, T.-T. B. Ngo, H. Dionne, L. F. Abbott, R. Axel, H. Tanimoto, G. M. Rubin, The neuronal architecture of the mushroom body provides a logic for associative learning. *eLife* **3**, e04577 (2014).
27. K. Ito, K. Suzuki, P. Estes, M. Ramaswami, D. Yamamoto, N. J. Strausfeld, The organization of extrinsic neurons and their implications in the functional roles of the mushroom bodies in *Drosophila melanogaster* Meigen. *Learn. Mem.* **5**, 52–77 (1998).
28. G. C. Turner, M. Bazhenov, G. Laurent, Olfactory representations by *Drosophila* mushroom body neurons. *J. Neurophysiol.* **99**, 734–746 (2008).
29. N. K. Tanaka, H. Tanimoto, K. Ito, Neuronal assemblies of the *Drosophila* mushroom body. *J. Comp. Neurosci.* **508**, 711–755 (2008).
30. D. Owald, J. Felsenberg, C. B. Talbot, G. Das, E. Perisse, W. Huettneroth, S. Waddell, Activity of defined mushroom body output neurons underlies learned olfactory behavior in *Drosophila*. *Neuron* **86**, 417–427 (2015).
31. R. Cohn, I. Morante, V. Ruta, Coordinated and compartmentalized neuromodulation shapes sensory processing in *Drosophila*. *Cell* **163**, 1742–1755 (2015).
32. C. Liu, P.-Y. Plaçais, N. Yamagata, B. D. Pfeiffer, Y. Aso, A. B. Friedrich, I. Siwanowicz, G. M. Rubin, T. Prete, H. Tanimoto, A subset of dopamine neurons signals reward for odour memory in *Drosophila*. *Nature* **488**, 512–516 (2012).
33. C. J. Burke, W. Huettneroth, D. Owald, E. Perisse, M. J. Krashes, G. Das, D. Gohl, M. Silies, S. Certel, S. Waddell, Layered reward signalling through octopamine and dopamine in *Drosophila*. *Nature* **492**, 433–437 (2012).
34. Y. Aso, A. Herb, M. Oguma, I. Siwanowicz, T. Templier, A. B. Friedrich, K. Ito, H. Scholz, H. Tanimoto, Three dopamine pathways induce aversive odor memories with different stability. *PLOS Genet.* **8**, e1002768 (2012).
35. T. Hige, Y. Aso, M. N. Modi, G. M. Rubin, G. C. Turner, Heterosynaptic plasticity underlies aversive olfactory learning in *Drosophila*. *Neuron* **88**, 985–998 (2015).
36. L. Y. McCurdy, P. Sareen, P. A. Davoudian, M. N. Nitabach, Dopaminergic mechanism underlying reward-encoding of punishment omission during reversal learning in *Drosophila*. *Nat. Commun.* **12**, 1115 (2021).
37. C. Huang, J. Luo, S. J. Woo, L. A. Roitman, J. Li, V. A. Pieribone, M. Kannan, G. Vasan, M. J. Schnitzer, Dopamine-mediated interactions between short- and long-term memory dynamics. *Nat.* **634**, 1141–1149 (2024).
38. K. Ueno, E. Suzuki, S. Nagano, K. Ofusa, J. Horiuchi, M. Saito, Coincident postsynaptic activity gates presynaptic dopamine release to induce plasticity in *Drosophila* mushroom bodies. *eLife* **6**, e21076 (2017).
39. C. E. Hancock, V. Rostami, E. Y. Rachad, S. H. Deimel, M. P. Nawrot, A. Fiala, Visualization of learning-induced synaptic plasticity in output neurons of the *Drosophila* mushroom body γ-lobe. *Sci. Reports* **12**, 10421 (2022).
40. N. Bielopolski, H. Amin, A. A. Apostolopoulos, E. Rozenfeld, H. Lerner, W. Huettneroth, A. C. Lin, M. Parnas, Inhibitory muscarinic acetylcholine receptors enhance aversive olfactory learning in adult *Drosophila*. *eLife* **8**, e48264 (2019).
41. E. Rozenfeld, H. Lerner, M. Parnas, Muscarinic modulation of antennal lobe GABAergic local neurons shapes odor coding and behavior. *Cell Rep.* **29**, 3253–3265.e4 (2019).
42. S. Israel, E. Rozenfeld, D. Weber, W. Huettneroth, M. Parnas, Olfactory stimuli and moonwalker SEZ neurons can drive backward locomotion in *Drosophila*. *Curr. Biol.* **32**, 1131–1149.e7 (2022).
43. E. Rozenfeld, M. Tauber, Y. Ben-Chaim, M. Parnas, GPCR voltage dependence controls neuronal plasticity and behavior. *Nat. Commun.* **12**, 7252 (2021).
44. E. Rozenfeld, N. Ehmann, J. E. Manoim, R. J. Kittel, M. Parnas, Homeostatic synaptic plasticity rescues neural coding reliability. *Nat. Commun.* **14**, 2993 (2023).
45. H. Lerner, E. Rozenfeld, B. Rozenman, W. Huettneroth, M. Parnas, Differential role for a defined lateral horn neuron subset in naïve odor valence in *Drosophila*. *Sci. Rep.* **10**, 6147 (2020).
46. P. F. Jacob, S. Waddell, Spaced training forms complementary long-term memories of opposite valence in *Drosophila*. *Neuron* **106**, 977–991.e4 (2020).
47. B. Zhao, J. Sun, Q. Li, Y. Zhong, Differential conditioning produces merged long-term memory in *Drosophila*. *eLife* **10**, e66499 (2021).
48. D. Pauls, J. E. R. Pfizenmaier, R. Krebs-Wheaton, M. Selcho, R. F. Stocker, A. S. Thum, Electric shock-induced associative olfactory learning in *Drosophila* larvae. *Chem. Senses* **35**, 335–346 (2010).
49. C. D. O. Beck, B. Schroeder, R. L. Davis, Learning performance of normal and mutant *Drosophila* after repeated conditioning trials with discrete stimuli. *J. Neurosci.* **20**, 2944–2953 (2000).
50. D. B. G. Akalal, C. F. Wilson, L. Zong, N. K. Tanaka, K. Ito, R. L. Davis, Roles for *Drosophila* mushroom body neurons in olfactory learning and memory. *Learn. Mem.* **13**, 659–668 (2006).

51. T. Zars, R. Wolf, R. Davis, M. Heisenberg, Tissue-specific expression of a type I adenylyl cyclase rescues the rutabaga mutant memory defect: In search of the engram. *Learn. Mem.* **7**, 18–31 (2000).
52. E. Bouzaiane, S. Trannoy, L. Scheunemann, P. Y. Plaçais, T. Preat, Two independent mushroom body output circuits retrieve the six discrete components of *Drosophila* aversive memory. *Cell Rep.* **11**, 1280–1292 (2015).
53. I. Cervantes-Sandoval, A. Martin-Peña, J. A. Berry, R. L. Davis, System-like consolidation of olfactory memories in *Drosophila*. *J. Neurosci.* **33**, 9846–9854 (2013).
54. D. Yu, D. B. G. Akalal, R. L. Davis, *Drosophila* α/β mushroom body neurons form a branch-specific, long-term cellular memory trace after spaced olfactory conditioning. *Neuron* **52**, 845–855 (2006).
55. M. J. Krashes, A. C. Keene, B. Leung, J. D. Armstrong, S. Waddell, Sequential use of mushroom body neuron subsets during *Drosophila* odor memory processing. *Neuron* **53**, 103–115 (2007).
56. A. L. Blum, W. Li, M. Cressy, J. Dubnau, Short- and long-term memory in *Drosophila* require cAMP signaling in distinct neuron types. *Curr. Biol.* **19**, 1341–1350 (2009).
57. S. Trannoy, C. Redt-Clouet, J. M. Dura, T. Preat, Parallel processing of appetitive short- and long-term memories in *Drosophila*. *Curr. Biol.* **21**, 1647–1653 (2011).
58. H. Qin, M. Cressy, W. Li, J. S. Coravos, S. A. Izzi, J. Dubnau, Gamma neurons mediate dopaminergic input during aversive olfactory memory formation in *Drosophila*. *Curr. Biol.* **22**, 608–614 (2012).
59. E. Perisse, D. Owald, O. Barnstedt, C. B. Talbot, W. Huettneroth, S. Waddell, Aversive learning and appetitive motivation toggle feed-forward inhibition in the *Drosophila* mushroom body. *Neuron* **90**, 1086–1099 (2016).
60. J. Séjourn, P. Y. Plaçais, Y. Aso, I. Siwanowicz, S. Trannoy, V. Thoma, S. R. Tedjakumala, G. M. Rubin, P. Tchéno, K. Ito, G. Isabel, H. Tanimoto, T. Preat, Mushroom body efferent neurons responsible for aversive olfactory memory retrieval in *Drosophila*. *Nat. Neurosci.* **14**, 903–910 (2011).
61. P. Y. Plaçais, S. Trannoy, A. B. Friedrich, H. Tanimoto, T. Preat, Two pairs of mushroom body efferent neurons are required for appetitive long-term memory retrieval in *Drosophila*. *Cell Rep.* **5**, 769–780 (2013).
62. J. H. Koenig, K. Saito, K. Ikeda, Reversible control of synaptic transmission in a single gene mutant of *Drosophila melanogaster*. *J. Cell Biol.* **96**, 1517–1522 (1983).
63. Y. Aso, G. M. Rubin, Dopaminergic neurons write and update memories with cell-type-specific rules. *eLife* **5**, e16135 (2016).
64. Y. Aso, I. Siwanowicz, L. Bräcker, K. Ito, T. Kitamoto, H. Tanimoto, Specific dopaminergic neurons for the formation of labile aversive memory. *Curr. Biol.* **20**, 1445–1451 (2010).
65. T. Boto, A. Stahl, X. Zhang, T. Louis, S. M. Tomchik, Independent contributions of discrete dopaminergic circuits to cellular plasticity, memory strength, and valence in *Drosophila*. *Cell Rep.* **27**, 2014–2021.e2 (2019).
66. M. Marquis, R. I. Wilson, M. Marquis, R. I. Wilson, Locomotor and olfactory responses in dopamine neurons of the *Drosophila* superior-lateral brain. *Curr. Biol.* **32**, 5406–5414.e5 (2022).
67. Y. Aso, D. Sitaraman, T. Ichinose, K. R. Kaun, K. Vogt, G. Belliart-Guirén, P.-Y. Plaçais, A. A. Robie, N. Yamagata, C. Schnaitmann, W. J. Rowell, R. M. Johnston, T.-T. B. Ngo, N. Chen, W. Korff, M. N. Nitabach, U. Heberlein, T. Preat, K. M. Branson, H. Tanimoto, G. M. Rubin, Mushroom body output neurons encode valence and guide memory-based action selection in *Drosophila*. *eLife* **3**, e04580 (2014).
68. J. A. Berry, A. Phan, R. L. Davis, Dopamine neurons mediate learning and forgetting through bidirectional modulation of a memory trace. *Cell Rep.* **25**, 651–662.e5 (2018).
69. N. C. Noyes, R. L. Davis, Innate and learned odor-guided behaviors utilize distinct molecular signaling pathways in a shared dopaminergic circuit. *Cell Rep.* **42**, 112026 (2023).
70. X. Zhang, N. C. Noyes, J. Zeng, Y. Li, R. L. Davis, Aversive training induces both presynaptic and postsynaptic suppression in *Drosophila*. *J. Neurosci.* **39**, 9164–9172 (2019).
71. J. A. Berry, I. Cervantes-Sandoval, M. Chakraborty, R. L. Davis, Sleep facilitates memory by blocking dopamine neuron-mediated forgetting. *Cell* **161**, 1656–1667 (2015).
72. J. Felsenberg, P. F. Jacob, T. Walker, O. Barnstedt, A. J. Edmondson-Stait, M. W. Pleijzier, N. Otto, P. Schlegel, N. Sharifi, E. Perisse, C. S. Smith, J. S. Lauritzen, M. Costa, G. S. X. E. Jefferis, D. D. Bock, S. Waddell, Integration of parallel opposing memories underlies memory extinction. *Cell* **175**, 709–722.e15 (2018).
73. J. Zeng, X. Li, R. Zhang, M. Lv, Y. Wang, K. Tan, X. Xia, J. Wan, M. Jing, X. Zhang, Y. Li, Y. Yang, L. Wang, J. Chu, Y. Li, Y. Li, Local 5-HT signaling bi-directionally regulates the coincidence time window for associative learning. *Neuron* **111**, 1118–1135.e5 (2023).
74. C. Prribbonow, Y. C. Chen, M. M. Heim, D. Laber, S. Reubold, E. Reynolds, I. Balles, T. F.-D. V. Alquicira, R. S. Grimalt, L. Scheunemann, C. Rauch, T. Matkovic, J. Rösner, G. Lichtner, S. R. Jagannathan, D. Owald, Postsynaptic plasticity of cholinergic synapses underlies the induction and expression of appetitive and familiarity memories in *Drosophila*. *eLife* **11**, e80445 (2022).
75. E. G. Govorunova, O. A. Sineshchekov, R. Janz, X. Liu, J. L. Spudich, Natural light-gated anion channels: A family of microbial rhodopsins for advanced optogenetics. *Science* **349**, 647–650 (2015).
76. R. I. Wilson, Neural networks for navigation: From connections to computations. *Annu. Rev. Neurosci.* **46**, 403–423 (2023).
77. D. Grover, J. Y. Chen, J. Xie, J. Li, J. P. Changeux, R. J. Greenspan, Differential mechanisms underlie trace and delay conditioning in *Drosophila*. *Nature* **603**, 302–308 (2022).
78. T. A. Ofstad, C. S. Zuker, M. B. Reiser, Visual place learning in *Drosophila melanogaster*. *Nature* **474**, 204–207 (2011).
79. C. Dan, B. K. Hulse, R. Kappagantula, V. Jayaraman, A. M. Hermundstad, A neural circuit architecture for rapid learning in goal-directed navigation. *Neuron* **112**, 2581–2599.e23 (2024).
80. A. M. M. Matheson, A. J. Lanz, A. M. Medina, A. M. Licata, T. A. Currier, M. H. Syed, K. I. Nagel, A neural circuit for wind-guided olfactory navigation. *Nat. Commun.* **13**, 4613 (2022).
81. A. Hamid, H. Gattuso, A. N. Caglar, M. Pillai, T. Steele, A. Gonzalez, K. Nagel, M. H. Syed, The conserved RNA-binding protein Imp is required for the specification and function of olfactory navigation circuitry in *Drosophila*. *Curr. Biol.* **5**, 473–488 (2024).
82. Y. Chen, R. Alfredson, D. Mottevalli, U. Stern, C.-H. Yang, Spatial learning in feature-impaired environments in *Drosophila*. *bioRxiv* 615625 [Preprint] (2024) <https://doi.org/10.1101/2024.09.28.615625>.
83. J. D. Seelig, V. Jayaraman, Neural dynamics for landmark orientation and angular path integration. *Nature* **521**, 186–191 (2015).
84. B. K. Hulse, H. Haberkern, R. Franconville, D. B. Turner-Evans, S. Y. Takemura, T. Wolff, M. Noorman, M. Dreher, C. Dan, R. Parekh, A. M. Hermundstad, G. M. Rubin, V. Jayaraman, A connectome of the *Drosophila* central complex reveals network motifs suitable for flexible navigation and context-dependent action selection. *eLife* **10**, e66039 (2021).
85. D. B. Turner-Evans, K. T. Jensen, S. Ali, G. M. Rubin, D. D. Bock, D. B. Turner-Evans, K. T. Jensen, S. Ali, T. Paterson, A. Sheridan, R. P. Ray, The neuroanatomical ultrastructure and function of a biological ring attractor. *Neuron* **108**, 145–163.e10 (2020).
86. R. Franconville, C. Beron, V. Jayaraman, Building a functional connectome of the *Drosophila* central complex. *eLife* **7**, e37017 (2018).
87. S. S. Kim, H. Rouault, S. Druckmann, V. Jayaraman, Ring attractor dynamics in the *Drosophila* central brain. *Science* **356**, 849–853 (2017).
88. Y. E. Fisher, J. Lu, I. D'Alessandro, R. I. Wilson, Sensorimotor experience remaps visual input to a heading-direction network. *Nature* **576**, 121–125 (2019).
89. J. Green, A. Adachi, K. K. Shah, J. D. Hirokawa, P. S. Magani, G. Maimon, A neural circuit architecture for angular integration in *Drosophila*. *Nature* **546**, 101–106 (2017).
90. D. Turner-Evans, S. Wegener, H. Rouault, R. Franconville, T. Wolff, J. D. Seelig, S. Druckmann, V. Jayaraman, Angular velocity integration in a fly heading circuit. *eLife* **6**, e23496 (2017).
91. H. Haberkern, S. S. Chitnis, P. M. Hubbard, T. Golet, A. M. Hermundstad, V. Jayaraman, Maintaining a stable head direction representation in naturalistic visual environments. *bioRxiv* 492284 [Preprint] (2022). <https://doi.org/10.1101/2022.05.17.492284>.
92. C. Lyu, L. F. Abbott, G. Maimon, Building an allocentric travelling direction signal via vector computation. *Nature* **601**, 92–97 (2022).
93. J. Lu, A. H. Behbahani, L. Hamburg, E. A. Westeinde, P. M. Dawson, C. Lyu, G. Maimon, M. H. Dickinson, S. Druckmann, R. I. Wilson, Transforming representations of movement from body- to world-centric space. *Nature* **601**, 98–104 (2022).
94. T. A. Currier, A. M. M. Matheson, K. I. Nagel, Encoding and control of orientation to airflow by a set of *Drosophila* fan-shaped body neurons. *eLife* **9**, e61510 (2020).
95. T.-W. Chen, T. J. Wardill, T. J. Wardill, Y. Sun, Y. Sun, S. R. Pulver, S. R. Pulver, S. L. Renninger, S. L. Renninger, A. Baohan, A. Baohan, E. R. Schreiter, E. R. Schreiter, R. A. Kerr, R. A. Kerr, M. B. Orger, M. B. Orger, V. Jayaraman, V. Jayaraman, L. L. Looger, L. L. Looger, K. Svoboda, K. Svoboda, D. S. Kim, D. S. Kim, Ultrasensitive fluorescent proteins for imaging neuronal activity. *Nature* **499**, 295–300 (2013).
96. T. Tully, T. Preat, S. C. Boynton, M. Del Vecchio, Genetic dissection of consolidated memory in *Drosophila*. *Cell* **79**, 35–47 (1994).
97. K. M. Scaplen, M. Talay, J. D. Fisher, R. Cohn, A. Sorkaç, Y. Aso, G. Barnea, K. R. Kaun, Transsynaptic mapping of *Drosophila* mushroom body output neurons. *eLife* **10**, e63379 (2021).
98. P. Masek, K. Worden, Y. Aso, G. M. Rubin, A. C. Keene, A dopamine-modulated neural circuit regulating aversive taste memory in *Drosophila*. *Curr. Biol.* **25**, 1535–1541 (2015).
99. M. E. Villar, M. Pavão-Delgado, M. Amigo, P. F. Jacob, N. Merabet, A. Pinot, S. A. Perry, S. Waddell, E. Perisse, Differential coding of absolute and relative aversive value in the *Drosophila* brain. *Curr. Biol.* **32**, 4576–4592.e5 (2022).
100. S. Sayin, J. F. De Backer, K. P. Siju, M. E. Wosniack, L. P. Lewis, L. M. Frisch, B. Gansen, P. Schlegel, A. Edmondson-Stait, N. Sharifi, C. B. Fisher, S. A. Calle-Schuler, J. S. Lauritzen, D. D. Bock, M. Costa, G. S. X. E. Jefferis, J. Gjorgjieva, I. C. Grunwald Kadow, A neural circuit arbitrates between persistence and withdrawal in hungry *Drosophila*. *Neuron* **104**, 544–558.e6 (2019).
101. S. Waddell, J. D. Armstrong, T. Kitamoto, K. Kaiser, W. G. Quinn, The amnesiac gene product is expressed in two neurons in the *Drosophila* brain that are critical for memory. *Cell* **103**, 805–813 (2000).

102. A. C. Keene, M. Stratmann, A. Keller, P. N. Perrat, L. B. Vosshall, S. Waddell, Diverse odor-conditioned memories require uniquely timed dorsal paired medial neuron output. *Neuron* **44**, 521–533 (2004).
103. Z. Okray, P. F. Jacob, C. Stern, K. Desmond, N. Otto, C. B. Talbot, P. Vargas-Gutierrez, S. Waddell, Multisensory learning binds neurons into a cross-modal memory engram. *Nature* **617**, 777–784 (2023).
104. P. T. Lee, H. W. Lin, Y. H. Chang, T. F. Fu, J. Dubnau, J. Hirsh, T. Lee, A. S. Chiang, Serotonin-mushroom body circuit modulating the formation of anesthesia-resistant memory in *Drosophila*. *Proc. Natl. Acad. Sci. U.S.A.* **108**, 13794–13799 (2011).
105. S. Dorkenwald, A. Matsliah, A. R. Sterling, P. Schlegel, S. Yu, C. E. McKellar, A. Lin, M. Costa, K. Eichler, Y. Yin, W. Silversmith, C. Schneider-Mizell, C. S. Jordan, D. Brittain, A. Halageri, K. Kuehner, O. Ogedengbe, R. Morey, J. Gager, K. Kruk, E. Perlman, R. Yang, D. Deutsch, D. Bland, M. Sorek, R. Lu, T. Macrina, K. Lee, J. A. Bae, S. Mu, B. Nehoran, E. Mitchell, S. Popovych, J. Wu, Z. Jia, M. A. Castro, N. Kemnitz, D. Ih, A. S. Bates, N. Eckstein, J. Funke, F. Collman, D. D. Bock, G. S. X. E. Jefferis, H. S. Seung, M. Murthy, The FlyWire Consortium, Neuronal wiring diagram of an adult brain. *Nature* **634**, 124–138 (2024).
106. Y. E. Fisher, M. Marquis, I. D'Alessandro, R. I. Wilson, Dopamine promotes head direction plasticity during orienting movements. *Nature* **612**, 316–322 (2022).
107. J. Green, V. Vijayan, P. Mussells Pires, A. Adachi, G. Maimon, A neural heading estimate is compared with an internal goal to guide oriented navigation. *Nat. Neurosci.* **22**, 1460–1468 (2019).
108. J. E. LeDoux, J. Moscarelli, R. Sears, V. Campese, The birth, death and resurrection of avoidance: A reconceptualization of a troubled paradigm. *Mol. Psychiatry* **22**, 24–36 (2017).
109. A. H. K. Wong, F. M. Wirth, A. Pittig, Avoidance of learnt fear: Models, potential mechanisms, and future directions. *Behav. Res. Ther.* **151**, 104056 (2022).
110. A. T. Kuan, G. Bondanelli, L. N. Driscoll, J. Han, M. Kim, D. G. C. Hildebrand, B. J. Graham, D. E. Wilson, L. A. Thomas, S. Panzeri, C. D. Harvey, W.-C. A. Lee, Synaptic wiring motifs in posterior parietal cortex support decision-making. *Nature* **627**, 367–373 (2024).
111. R. Mohandasan, M. Thakare, S. Sunke, F. M. Iqbal, M. Sridharan, G. Das, Enhanced olfactory memory detection in trap-design Y-mazes allows the study of imperceptible memory traces in *Drosophila*. *Learn. Mem.* **29**, 355–366 (2022).
112. B. Zhao, J. Sun, X. Zhang, H. Mo, Y. Niu, Q. Li, L. Wang, Y. Zhong, Long-term memory is formed immediately without the need for protein synthesis-dependent consolidation in *Drosophila*. *Nat. Commun.* **10**, 4550 (2019).
113. P. Schlegel, Y. Yin, A. S. Bates, S. Dorkenwald, K. Eichler, P. Brooks, D. S. Han, M. Gkantia, M. dos Santos, E. J. Munnely, G. Badalamente, L. S. Capdevila, V. A. Sane, A. M. C. Fragniere, L. Kiassat, M. W. Pleijzier, T. Stürner, I. F. M. Tamimi, C. R. Dunne, I. Salgarella, A. Javier, S. Fang, E. Perlman, T. Kazimiers, S. R. Jagannathan, A. Matsliah, A. R. Sterling, S. Yu, C. E. McKellar, F. Consortium, M. Costa, H. S. Seung, M. Murthy, V. Hartenstein, D. D. Bock, G. S. X. E. Jefferis, Whole-brain annotation and multi-connectome cell typing of *Drosophila*. *Nature* **634**, 139–152 (2024).
114. E. Perisse, Y. Yin, A. C. Lin, S. Lin, W. Huettneroth, S. Waddell, different kenyon cell populations drive learned approach and avoidance in *Drosophila*. *Neuron* **79**, 945–956 (2013).
115. F. Li, J. Lindsey, E. C. Marin, N. Otto, M. Dreher, G. Dempsey, I. Stark, A. S. Bates, M. W. Pleijzier, P. Schlegel, A. Nern, S. Takemura, N. Eckstein, T. Yang, A. Francis, A. Braun, R. Parekh, M. Costa, L. Scheffer, Y. Aso, G. S. X. E. Jefferis, L. F. Abbott, A. Litwin-Kumar, S. Waddell, G. M. Rubin, The connectome of the adult *Drosophila* mushroom body provides insights into function. *eLife* **9**, e62576 (2020).
116. K. M. Scaplen, M. Talay, K. M. Nunez, S. Salamon, A. G. Waterman, S. Gang, S. L. Song, G. Barnea, K. R. Kaun, Circuits that encode and guide alcohol-associated preference. *eLife* **9**, e48730 (2020).
117. S. Heinze, U. Homberg, Maplike representation of celestial E-vector orientations in the brain of an insect. *Science* **315**, 995–997 (2007).
118. M. Parnas, A. C. Lin, W. Huettneroth, G. Miesenböck, Odor discrimination in *Drosophila*: From neural population codes to behavior. *Neuron* **79**, 932–944 (2013).
119. J. E. Manoim, A. M. Davidson, S. Weiss, T. Hige, M. Parnas, Lateral axonal modulation is required for stimulus-specific olfactory conditioning in *Drosophila*. *Curr. Biol.* **32**, 4438–4450.e5 (2022).
120. Eyal-ro/Rosenfeld-et-al-2025: Zenodo-version. doi: 10.5281/ZENODO.13764295.

**Acknowledgments:** We thank A.-S. Chiang, M. Siles, and the Bloomington Stock Center for fly strains. **Funding:** This work was supported by the Israel Science Foundation (ISF, 404/23 to M.P.), the United States–Israel Binational Science Foundation (BSF, 2019026 and 2020636 to M.P.), and the European Research Council (ERC, 101085605 to M.P.). **Author contributions:** E.R.: Writing—original draft, conceptualization, investigation, writing—review and editing, methodology, resources, data curation, validation, supervision, formal analysis, software, and visualization. M.P.: Writing—original draft, conceptualization, writing—review and editing, methodology, resources, funding acquisition, data curation, validation, supervision, formal analysis, project administration, and visualization. **Competing interests:** The authors declare that they have no competing interests. **Data and materials availability:** The data and code used to generate the figures in this manuscript are available in the following repository: <https://zenodo.org/records/13764295>. (120). All data needed to evaluate the conclusions in the paper are present in the paper and/or the Supplementary Materials.

Submitted 7 May 2024

Accepted 30 October 2024

Published 6 December 2024

10.1126/sciadv.adq3016